Journal of Alloys and Compounds 798 (2019) 714–740

Contents lists available at ScienceDirect

Journal of Alloys and Compounds

journal homepage: http://www.elsevier.com/locate/jalcom

Review

Review of the methodologies used in the synthesis gold nanoparticles by chemical reduction

Carla Daruich De Souza*, Beatriz Ribeiro Nogueira, Maria Elisa C.M. Rostelato

Instituto de Pesquisas Energéticas e Nucleares Avenida Professor Lineu Prestes, 2242, Cidade Universitária, São Paulo SP, 05508-000, Brazil

ARTICLE INFO

Article history:
Received 6 February 2019
Received in revised form
9 May 2019
Accepted 13 May 2019
Available online 28 May 2019

Keywords:
Gold nanoparticles
Gold nanoparticles synthesis
Gold nanoparticle review
Chemical reduction

ABSTRACT

This paper presents a review in gold nanoparticles focusing on chemical reduction synthesis mechanisms. We hope to aid students and researchers starting in the nanotechnology field by compiling the most used synthesis methods, so they can select the ones that best suit them. The compiled information in this paper approached the following methods: Turkevich Method; Synthesis with $NaBH_4$ with/without citrate; Seeding- Growth; Synthesis by Ascorbic Acid; Green Synthesis; Brust-Schiffrin; and synthesis using other reducing agents. Papers that had clear synthesis information were selected for this work, but that doesn't mean they were synthesis focused. Over 150 papers were analyzed. After compiling the information for these papers, we can conclude that nanoscience is revolutionizing all the areas that are applied to.

Contents

1. Introduction

Nanoscience is the study of particles, structures and materials

* Corresponding author.
E-mail addresses: carladdsouza@yahoo.com.br (C. Daruich De Souza), bia.ribnog@gmail.com (B. Ribeiro Nogueira), elisaros@ipen.br (M.E.C.M. Rostelato).

https://doi.org/10.1016/j.jallcom.2019.05.153
0925-8388/

that are in the nanoscale (nm) and have unique properties. Their configuration in the nanometric size promotes alteration in their physical, chemical, and biological behaviors. The quantum confinment effects states that the properties of materials are size-dependent in this scale range. In nanomaterials, the energy levels of the electrons are not continuous as when compared to the bulk form. They are discrete due to the confinement of the electronic wave function in up to three physical dimensions. That leads to a change in surface area and electron confinment, makes the change in materials properties. For example, properties such as melting point, fluorescence, electrical conductivity, magnetic permeability, and chemical reactivity change as a function of the size of the particle [1–3].

Maybe the most important result of the nanoscale quantum effects is the ability to tune the properties [4,5]. It means that a researcher can change the proprieties behavior to serve a determined propose. For example, changing the fluorescence color of a particle can be used to identify diseases [1].

Michael Faraday provided the first description, in scientific terms, of the optical properties of nanometer-scale metals in his 1857 paper describing the production of colloidal gold by the reduction of chloroauric acid by phosphorous [6].

This paper will present different chemical synthesis methods for producing gold nanoparticles. They have all sort of different applications in several fields such as in industry, electronics, and environmental sciences [1,7–13]. Gold nanoparticles are the type most reported in the literature. Around 87,000 papers were published since 1996. Copper, Silver, Iron and titanium nanoparticles are also extensively reported (85, 57, 59, 36 thousand publications, respectively) and are worth a review of their own. According with Alves, the most used synthesis pathway is by chemical reduction (around 53,000 of the 87,000 used chemical reduction). That will be the focus of this review. Other synthetic methods include electrochemical [14], sonochemical [15], thermal [16] or photochemical [17] reduction techniques, and ionic liquids [18].

Gold nanoparticles (AuNPs) applications are shape and size dependent. As examples: gold nanorods are being used as biosensors and to kill cancer cells [19,20] and drug delivery [21,22]. Nanobubbles containing gold nanoparticles can reach a determined affected area and burst due to increase heat from a laser beam or infrared rays. They them slowly penetrate the cancer cell wall inhibiting growth (Golden Bullet Technique) [23].

Their interaction with light is also environment, size and physical dimensions dependent. Consistent with the Fermi liquid model, plasmons are explained as a negatively charged electron cloud coherently displaced from its equilibrium position around a lattice made of positively charged ions [24]. When a small spherical gold nanoparticle is exposed to light, the oscillating electric field causes the conduction electrons to oscillate coherently. Because of the displacement of the electron cloud, a restoring force arises from Coulomb attraction between electrons and nuclei resulting in oscillation of the electron cloud relative to the nuclear framework [25]. The interactions in NPs with size much smaller than photon wavelength are non-propagating excitations, called localized surface plasmons (LSPs), due to the resulting plasmon oscillation being distributed over the entire particle volume. Such a coherent displacement of electrons from the positively charged lattice generates the restoring force that pulls the polarized electrons back to the lattice. When the wavelength is greater than the size of the NPs, a uniform and oscillating electric field is formed resulting in an in-phase electrons oscillation. Nevertheless, this collective oscillation is constrained by the reduced dimensions of the NP in which the electrons are confined, leading to a significant absorption of the wavelengths around green. That is why AuNPs appear with the complementary color, which is red [2,7,12,26].

The color change is also seen when excess salt is added to the gold solution. The surface charge of the gold nanoparticle becomes neutral, causing nanoparticles to aggregate. As a result, the solution color changes from red to blue. To minimize aggregation, it might be necessary to use coating agents in the surface, such as polymers, small molecules, and biological recognition molecules. This surface modification enables gold nanoparticles to be used extensively in chemical, biological, engineering, and medical applications [7,27,28].

Some examples of the use of gold nanoparticles in medical applications are:

- Therapeutic Agent Transport: The large ratio of surface area-volume of gold nanoparticles enables their surface to be coated with hundreds of molecules (including ligands, antibodies, and therapeutic, diagnostic and targeting agents) [29,30].
- Photodynamic Therapy: Heat can be generated by gold nanoparticles when excited by light with 700–800 nm wavelengths. When positioned inside a tumor, the particles rapidly heat up, killing tumor cells [31,32].
- Sensors: Gold nanoparticles can be used in Raman spectroscopy as substrates to enable/improve measurements of vibrational energies of chemical bonds. This strategy can be used for proteins detection [33].
- Probes: In dark-field microscopy, gold nanoparticles can produce an array of colors that can be used for biological imaging applications [34].
- Diagnostics: Gold nanoparticles are also used to detect biomarkers in the diagnosis of heart diseases, cancers, and infectious agents [35].
- Treatment: gold nanoparticle can be used to improve the radiation therapy dose delivery or can be used for treatment when activated to gold-198 [36].

Most of the nanoparticle products being investigated are still in the development stage. For example, the gold-198 nanobrachyseeds are mostly in the dosimetry simulation stage and at the animal tests studies. Human testing, toxicity evaluations, hospital planning dosimetry computer programs, delivery systems, and training aren't yet being developed. A few rare examples are: AuroVist™ used as contrast for Computed Tomography [37] and Ni-NTA-Nanogold®, designed a marker to locate proteins in electron microscopy [38].

2. Chemical Phenomena's and their role in nanoparticle formation

The synthesis of AuNPs by chemical reduction contains two major steps:

- the use of reduction agents such as borohydrides, citric and oxalic acids, polyols, hydrogen peroxide, sulfites, among many others. They provide electrons to reduce the gold ions, Au^{3+} and Au^{+} to Au^{0} which is the electric state for nanoparticles;
- the use of stabilization agents such as trisodium citrate dihydrate, sulfur ligands (mostly thiolates), phosphorus ligands, polymers, surfactants (in particular cetyltrimethylammonium bromide, CTAB), and others [39]. They stabilize nanoparticles against aggregation by imputing a repulsive force that control growth of the nanoparticles in terms of rate, final size or geometric shape. It is possible that stabilizing agent is the same molecule that acts as the reduction agent [40].

Functionalization is also available in the design of nanoparticles

for a particular usage. For instance, a target molecule can be attached to the AuNPs surface to increase intake in a particular organ.

Nanoparticle synthesis is extremely sensitive to multiple factors. A simple unwashed pipet tip may add foreign material enough to displace the stabilizing agent causing aggregation. Acidic or basic solutions can change the average diameter and size distribution by increasing dissolution rate to ionic form that can re-deposit onto existing nanoparticles.

Another important question is that size and shape can influence function. As an example, Schleh et al. [41]. discovered that size and surface charge of gold nanoparticles determine absorption across intestinal barriers and accumulation in secondary target organs after oral administration.

In the next items, we will summarize a few chemical phenomena's and their role in nanoparticle formation.

2.1. Characteristics dependence

The formation, size, shape, and function of the AuNPs is highly influenced by the physical and chemical characteristics of their synthesis. Reaction temperature, stirring rate, the ratio of gold to reducing agent are some of those constraints [42].

As an example, in the Turkevich method, trisodium citrate acts as a reducing agent and citrate binds to the nanoparticle surface acting as a weak stabilizer. Trisodium citrate is also a weak base, changing the reaction pH. Since the reactivity of the gold complexes, reflected by their reduction potential, changes when pH varies, the citrate concentration will influence the final outcome [43]. An example is presented by Ji et al. (reference [43]). Fig. 1 presents the size variation of gold nanocrystals through standard citrate reduction in boiling water. The molar ratio between trisodium citrate and choroauric acid was varied [40]. Another example using Frens reaction variation can be found in Ref. [40].

2.2. Surface charge

Since large fraction of atoms is concentrated at the nanoparticle surface, the region has a major influence in its chemical and physical properties. Because the surface atoms exhibit incomplete valence, being only bound to the internal atoms, their external sites are open for interaction with donor-acceptor species, or ligands (similar behavior as their related metal complexes) [42].

Most applications require the stabilization of the nanoparticles as colloidal dispersions through surface modification with appropriate coordinating species, such as citrate ions, thiols, or surfactants. It creates the possibility of controlling the stability of the dispersions by exploiting the charge and steric properties of the metal complexes, while modifying nanoparticles function [42].

The AuNPs properties is due to a large percentage of surface atoms and their delocalized electrons which behave as plasmon waves. The coordination sites of the surface atoms are not complete, allowing the binding of donor-acceptor species, or ligands. In solution, molecules associate with the nanoparticle surface and these surface bound molecules establish a double layer of charge that prevents nanoparticle aggregation. Also, particles can be functionalized with molecules that 'flip' the surface charge from negatively charged gold nanoparticles to a positively charged surface. This coating agent can also be functionalized to provide reactive groups, such as amines, for subsequent modification [42].

The surface of most nanoparticles is dynamic and is strongly influenced by the local environment. Different conditions will affect the particle in different ways. High salt environments will collapse the double layer and cause nanoparticle aggregation. Proteins and other biomolecules will often associate with and stabilize particles [42].

To access the stabilization, zeta potential assessment should be performed. Typically, nanoparticles with zeta potentials values outside of the 20 to −20 mV range have sufficient electrostatic repulsion to remain stable in solution.

2.3. Surfactants

Surfactants have ability to control the crystal growth of nanomaterials to achieve desired morphologies [44]. They are amphiphilic substances that, when present at low concentration, have property of adsorbing on surfaces or interfaces resulting in an alteration of free energy available. This property makes surfactants

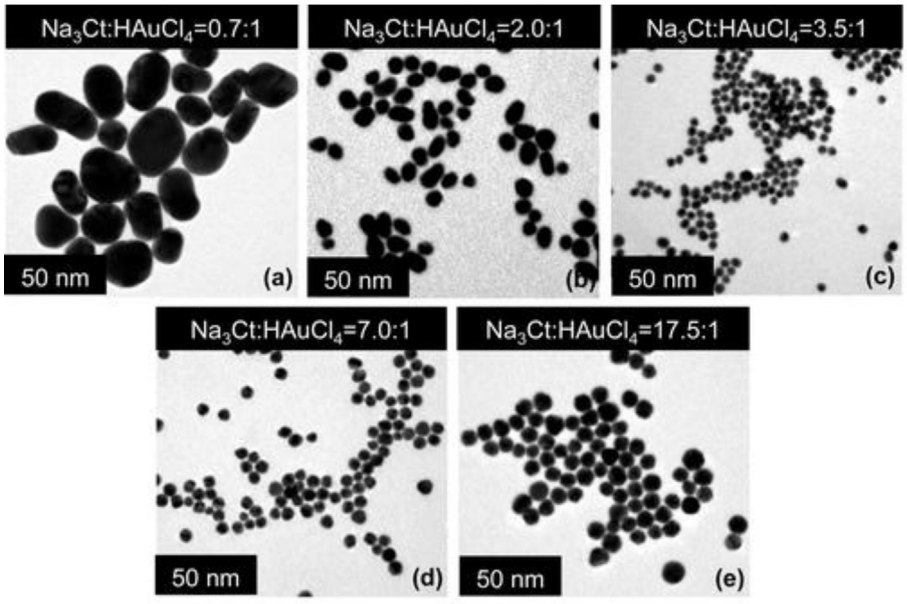

Fig. 1. TEM images a-e of gold nanocrystals synthesized with different sodium citrate/$HAuCl_4$ ratios. Published by Ji et al. [43]. "Reprinted with permission from Ji et al. [43]. Copyright (2019) American Chemical Society".

a very interesting option to be used as surface coating in nanoparticles. They are being extensively explored as a simple, effective and economical method. In contrast to their bare counterparts, the surfactant coated nanoparticles remain well dispersed in relatively dilute solutions. When higher concentrations of surfactant NPs are deposited on a smooth solid surface, they display a strong propensity to self-assemble into ordered arrays [45].

Very small nanoparticles with narrow size dispersion can be prepared using a two-phase process in the presence of organic thiols. For example, in the method proposed by Brust et al. [46], the gold salt is dissolved in water and first transferred to the organic phase using a suitable phase-transfer agent, such as tetraoctylammonium bromide (TOAB). Then, an aqueous sodium borohydride solution is added to the stirred biphasic system, leading to the formation of gold nanoparticles, changing the organic phase color from the characteristic orange to red or brown, depending on the size. The ratio of gold to organo-thiol and the reaction temperature control particle size. The nanoparticles, protected by a compact shell of organo-thiols, are stable for long periods of time, either in solution or as solids that can be readily redispersed in organic solvents [42]. Fig. 2 shows the different morphology of nanoparticles synthetized with different surfactants elucidating the surfactants impact in overall morphology.

2.4. Functionalization and stabilizers

Chemisorption, electrostatic attraction or hydrophobic interaction can attach a molecule to a NP surface, most commonly provided by a head group of the ligand molecule. Various chemical functional groups have a possibility to bind to inorganic surfaces, such as thiol to gold [5]. For example, gold nanoparticles in an aqueous solution synthesized by citrate reduction results in negatively charged citrate ions adsorbed on their surface and are thus stabilized by electrostatic repulsion. This weak-bind citrate layer can be replaced by ligands binding stronger to the particle surface [40].

In this ligand-exchange strategy, the molecules stabilizing the particles in the original first phase are replaced by other, more strongly binding ligands that allow the transfer to the second phase and provide colloidal stability or new function [40].

The protection against aggregation can be achieved by attaching an inert molecular chain (such as polyetilene glycol-PEG) or functional groups that have terminating linear molecules. In water-soluble nanoparticles, such as the AuNPs, these functional groups are often carboxylic acids that uses electrostatic repulsion to provide stabilization (this can be exploited in the conjugation of other molecules) [40].

All modification performed requires that the new version is fully re-characterized. A great deal of work will be necessary to adjust the quantities of each solution. Further purification, centrifugation, adjustment, or manipulation may be necessary.

3. Objectives

For newcomers in the nanotechnology field it will be clear that reproducing literature methods do not, in most cases, yield comparable, or even acceptable, results. Since we are in the nanoscale, several issues, such as reagent, glassware, and equipment calibration, will play a major role in the results obtained. This review will present relevant journal articles that approach gold nanoparticles synthesis mechanisms by chemical reduction. Papers that had clear synthesis information were selected, but that doesn't mean they were synthesis focused. We expect that this review will help students and researchers starting in the nanotechnology field by compiling the most used synthesis methods, so they can select the ones that best suit them. We encourage the reader, after the selection of the parts of interest, to read the brilliant original papers featured in this review.

The compiled information was prepared during September 2017–November of 2018 and classic search engines were used such as Science Direct, ACS (American Chemical Society), Elsevier, PubMed, Google Academics, among others.

A basic search with the words ***Gold Nanoparticles, synthesis*** shows the incredible increase of research articles published in the field. The number doubled in 5 years period (2013–2018), reflecting the intense attention that this field is receiving (Fig. 3).

4. Synthesis

Oxidation states of gold include Au^{+1} (aurous), Au^{+3} (auric), and its non-oxidized state Au^0. The Au^0 is the final desirable state for nanoparticles. So, the major step involving the synthesis of AuNPs is reducing Au^{+1} or Au^{+3} to Au^0 by adding an electron donor (reduction agent) in the reaction. The precursor of choice for the majority of researchers is chloroauric acid, $HAuCl_4$ with gold in its Au^{+3} oxidation states [2,47].

Since the $HAuCl_4$ is corrosive, glass or plastic spatula must be used avoiding contact with metal. In the preparation of gold nanoparticles, cleaning of glassware is very crucial. Thus, all the glassware and magnetic stirrer should be thoroughly cleaned with aqua regia and then rinse with nanopure water and dried. This step will avoid aggregation of residual gold particle and unwanted nucleation during synthesis procedures. All the gold nanoparticles batches must be stored in the dark to minimize the photo induced

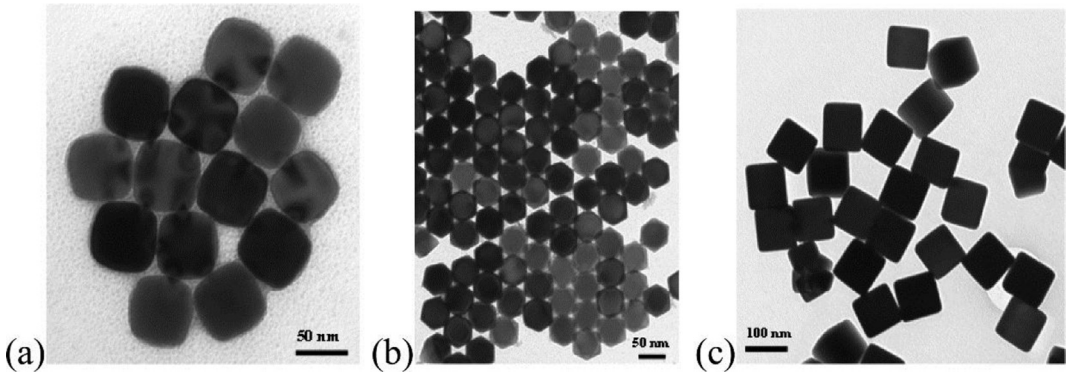

Fig. 2. TEM images (a–c) of different nanoparticles synthetized with different surfactant (cadmium sulfide) concentration. Published by Bakshi et al. [44]. "Reprinted with permission from Bakshi et al. [44]. Copyright (2019) American Chemical Society."

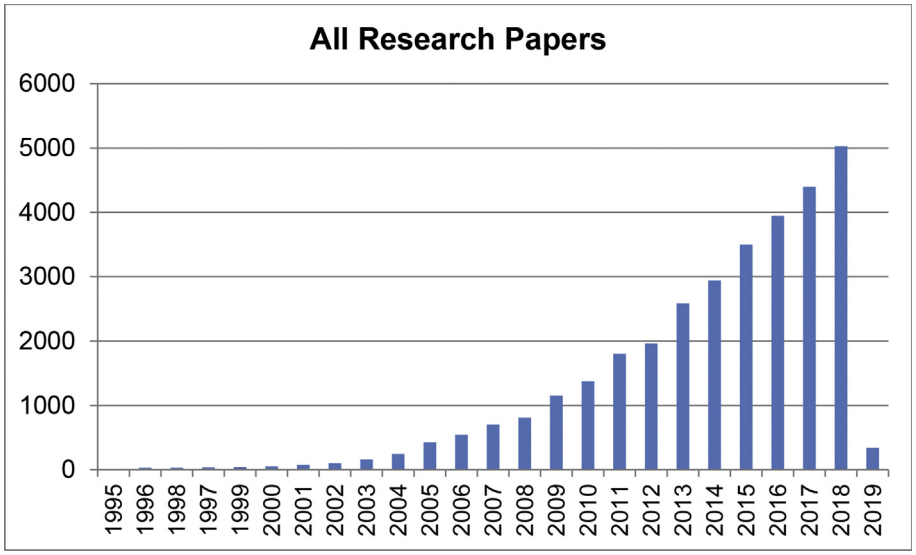

Fig. 3. Number of research articles published between 1995 and 2019 (the publications for 2019 are only in the accepted stage).

oxidation and preferably inside a refrigerator to diminish heat influence. Nano pure water is obtained by purification systems that yield low values (<1 ppb) of TOC (total organic carbon). This index is used as a non-specific indicator of water quality or cleanliness of pharmaceutical manufacturing equipment.

Although some other forms are used (see some examples in section 2.7), by far, the most used gold reagent used in nanoparticle synthesis is $HAuCl_4$. Most researchers purchase it ready to use. $HAuCl_4$ can also be obtained from gold foils by a simple method. Needless to state that the higher the gold purity (usually 99% or greater) purer the final product will be. Aqua Regia, a mixture of HCl and HNO_3, dissolves gold. Neither HCl nor HNO_3 can achieve this alone because, in combination, each have different function. Nitric acid, HNO_3, is a powerful oxidant that dissolves minimum amounts of gold, forming Au^{3+} ions. The hydrochloric acid, HCl, provides chloride ions (Cl^-), which react with the gold ions to create tetrachlorourate (III) anions, also in solution. The reaction with hydrochloric acid is an equilibrium reaction that favors the formation of chlorourate anions ($AuCl^{4-}$). This results in removal of ions from the gold of solution oxidation of remaining gold [48].

$$Au + HNO_3 + 4HCl \leftrightarrow AuCl_4^- + NO_2 + H_3O^+ + 2H_2O$$

Removal of the residual nitric acid can be carried out by repeated heating with the addition of hydrochloric acid. The process presented below is a modified process (from the literature [49]) that we use in our laboratory:

1. About 0.7 g of gold metal is placed in a 250 mL beaker. Seventy milliliters of aqua regia (HCl and HNO_3 in a volume ratio of 3:1) are added slowly;
2. The mixture is stirred and gradually heated to 50 °C. When gold dissolution is finished (about 1 min), the temperature is gradually raised to 70–80 °C;
3. The solution is continuously heated until it is concentrated to 30 mL.
4. HCl is added slowly to the hot solution until the brown nitric vapors are completely eliminated. The final volume reached is about 40 mL.
5. The solution is kept under heat until it is concentrated to 30 mL;
6. The procedure described in items 4 and 5 is repeated 3 times until no brown nitric vapor is formed. The presence of acid vapors is verified by pH indicator;
7. The solution is concentrated (by heating) to 15 mL;
8. Chlorouric acid in liquid form is ready for use.

Faraday [6] presented the first synthesis methodology. For AuNPs production, a saturated solution of white phosphorus in freshly distilled diethyl ether was diluted with three times its volume of diethyl ether. Fifty milliliters of chloroauric acid solution (50 mg of Au) was diluted with 45 mL of distilled water and with 5 mL of 0.1 N KOH. This solution was treated, using good mechanical stirring, in one case with 1.0–2.0 mL of the phosphorus-ether solution. The solution turned first brown, then grey, purple and red, finally giving a deep-red product. The product has heated to boiling and a stream of filtered air was drawn through it in order to oxidize any remaining phosphorus. Electron microscopic examination revealed extremely fine particles with a mean diameter of 5 nm.

Since the basic methodology for producing AuNPs is well established, the new research trends [40] are in using different stabilizers (thiols [50], organic molecules [51,52], polymers [53]), different coating agents (polymers [54–56], organic ligands [57,58], and even other metals [59–61]). Different synthesis methods using microwave [62], UV [63], and radiation [64,65], among others [66], are also under development. Investigation on the nanoparticle and its different uses is currently ongoing [67–69].

Nanoparticles are generally produced by reducing tetrachloroauric acid with various agents such as borohydride, amines, alcohols, carboxylic acids, sodium citrate, sodium borohydride, ascorbic acid, and others [36,53]. At the same time, small organic molecules or polymers should/can be added to the system to prevent the aggregation of the formed nanoparticles. The final shape achieved is generally spherical [70].

The following review presents papers with well described original synthesis. Papers that state “synthesis reported elsewhere” or similar, the original papers were tracked and evaluated.

The criteria for being mentioned in this review were: relevancy with keywords and have complete original synthesis description.

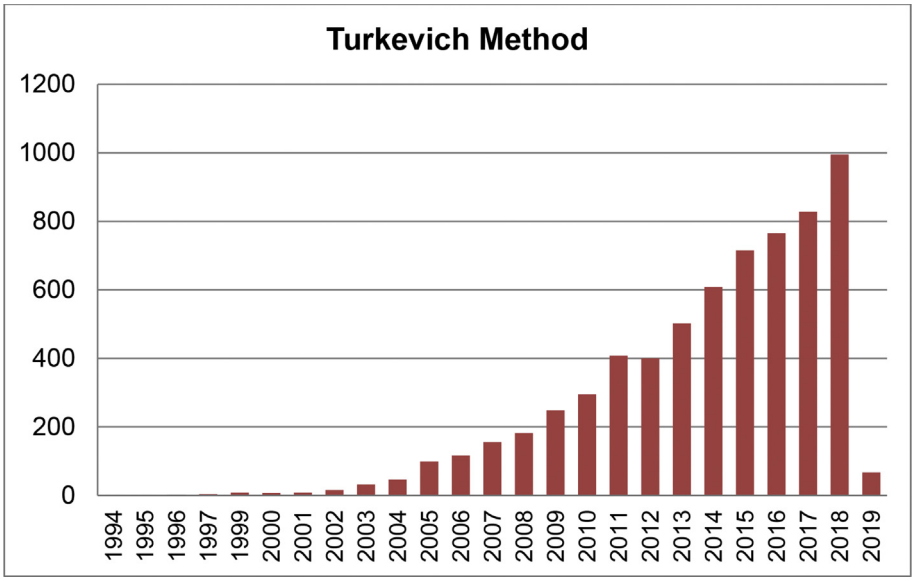

Fig. 4. Number of research articles published using the Turkevich between 1995 and 2019.

4.1. Synthesis with citrate – the Turkevich Method

Search key words: sodium citrate; nanoparticles; gold.

Fig. 4 presents the amount of published papers for the Turkevich method.

The classical, well described, synthesis method was presented by Turkevich in 1951 [71] using trisodium citrate (cited mostly as sodium citrate, also as Na_3citrate, Na-cit, Nacit or simply citrate) as a reducing agent. The publication resulted in several others with some differences to the basic method presented. Mainly, the variations involve $HAuCl_4$/sodium citrate ratio, pH control and temperature influence in nanoparticle size and stabilization.

The following theory is explained by Polte [72]. Colloidal stability is reached because the aggregation barrier (activation energy that two particles have to overcome to merge into one) increases with an optimum particle size. The process is summarized in Fig. 5.

In the first step of nanoparticle formation, the high reduction rate increases the number of particles rapidly forming clusters with 1–2 nm. In the second step, reduction continues, but at a much lower rate, and the freshly formed particles that are likely to have a weak stabilization undergo coalescence processes (coalescence is the process by which two or more droplets, bubbles or particles merge during contact to form a single daughter droplet, bubble or particle) leading to a decrease in the number of particles. When the particle size reaches a mean radius of about 2.5 nm, the number of particles remains constant, but particles keep growing in size. Taking the polydispersity into account, the smaller particles in that size distribution have radii of around 1.5 nm [72].

Subsequently, the AuNPs grow due to the diffusion of the gold atoms reduced in solution. Hence, a diffusional growth comprises the third step of the growth process which further decreases the polydispersity. When the particles reach a radius of around 4–5 nm, the growth rate increases drastically and the remaining 70–80% of the gold salt is reduced rapidly. In this fourth step, particle size increases to the final radius [72]. TEM image is shown on Fig. 6.

The ruby red color of the final colloid represents the state without any gold ions in solution. Fig. 7 show our gold nanoparticle reaction color change (performed with sodium citrate).

Table 1 presents a summary of the papers presented in this

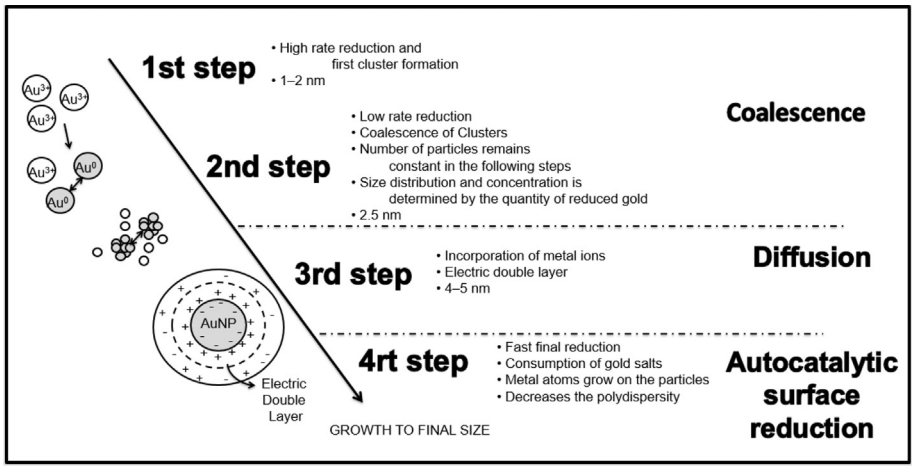

Fig. 5. Gold Nanoparticle formation steps.

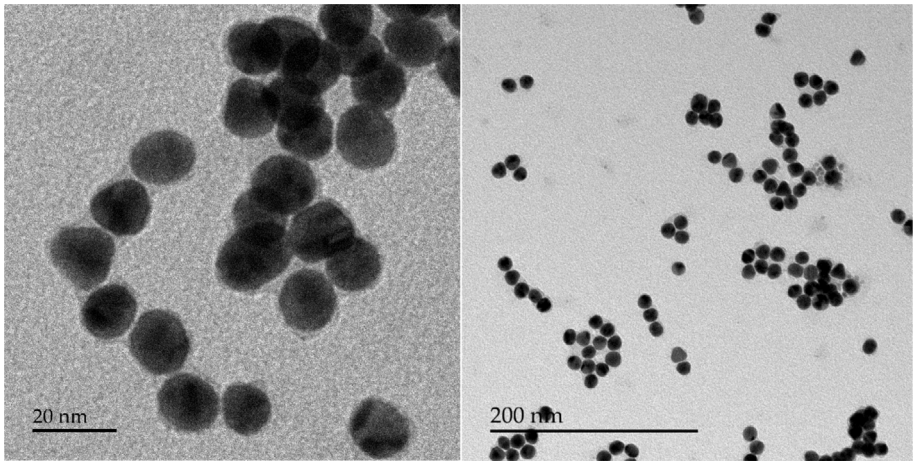

Fig. 6. TEM images for citrate capped AuNP. Notice the good size distribution [11].

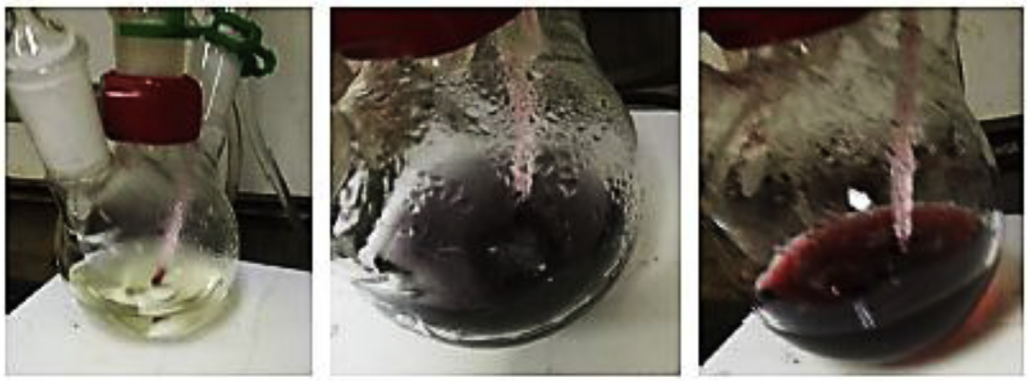

Fig. 7. Typical color change in gold nanoparticle synthesis [11]. *print in color*. (For interpretation of the references to color in this figure legend, the reader is referred to the Web version of this article.)

section (the term et al. was suppressed).

Turkevich method for sodium citrate is as follows: 95 mL of $HAuCl_4$ solution (containing 5 mg Au) were heated to the boiling point and 5 mL of 1% sodium citrate solution was added to the boiling solution with good mechanical stirring. The reaction mixture was colorless for 12 s after the addition of the citrate, and then it turned purpleish-blue within a fraction of a second. After 5 min, the final color was deep wine red. The best results were obtained with 5–50 mg citrate addition. The particle size achieved 20 nm [71].

Frens [73] reported that a 50 mL with 0.2% boiling solution of $HAuCl_4$ mixed for 5 min with 0.5 mL of 1% sodium citrate yielded nanoparticles with 16 nm. The colors vary from faintly blue to red.

Gold nanoparticles were prepared by Yonezawa with a modified citrate-reduction process. Into refluxing water (250 mL) in a 500 mL round-bottom, scratch-free flask, that had been washed with a commercial detergent and water, $HAuCl_4$ (5.8 mM, 25 mL) was added and the solution was heated to boiling. Then, a mixed solution (25 cm^3) of the stabilizer sodium 3-mercaptopropionate and sodium citrate (2.0%) was injected. The color of the solution turned from yellow to red or brown. The best results were obtained with stabilizer/gold ratio of 0.1 [74]. Average particle size was 10 nm.

Zhang et al. [75] prepared the aqueous gold nanoparticles, by addition of 4 mL of 1% sodium citrate to 100 mL of 0.01% boiling $HAuCl_4$ solution. The mixture was stirred until a deep wine-red color was obtained, indicating formation of gold nanoparticle suspension with 10 nm in size.

Gold nanoparticles were prepared by Mine et al. [76] by reduction of gold salt with sodium citrate [25]. Freshly prepared 0.94 mL of 0.34 M sodium citrate in H_2O was added to 200 mL of 0.24 mM $HAuCl_4$ in H_2O at a constant temperature of 80 °C under vigorous stirring. The color of the mixture turned wine red within a few minutes, which indicates the presence of Au nanoparticles [26]. The particles were 15 nm in average.

Seitz et al. prepared gold nanoparticle by adding 40 mL of 0.5 M $HAuCl_4$ solution to 10 mL of distilled water under reflux and stirring. The resulting $HAuCl_4$ solution has a concentration of 2×10^{-3} M. Sodium citrate (0.5 M, 160 mL) in water is added to 10 mL of water, resulting in a concentration of 8×10^{-3} M. This solution (10 mL) is added to the boiling $HAuCl_4$ solution. The mixture of $HAuCl_4$ and sodium citrate was refluxed for 1 h. The resulting grey mixture turned slowly to a light red color. After boiling for 1 h, the solution was left to cool at room temperature. The AuNPs were wine red and presented 40 nm [77].

Yang et al. method used: 4 mL, 24.3 mM of $HAuCl_4$–ethanol solution added into a boiling solution of tri-sodium citrate (100 mL of 1.0 mM) with rapid stirring. After the solution turning purple red within 30 s, it was cooled quickly in the ice-bath and concentrated to 20 mL in vacuum. Particle size was 4 nm [78].

Gold nanoparticles used by Huang et al. in a 1 L round-bottom flask equipped with a condenser, 500 mL of 1 mM $HAuCl_4$ was brought to a rolling boil with vigorous stirring in an oil-bath. After

Table 1
Summary of the papers presented for the Turkevich.

Turkevich method				
Reference		$HAuCl_4$ (concentration of $HAuCl_4$/volume - solvent used)	Citrate (concentration in water or mass of citrate added)	AuNP size
Turkevich [71]		5 mg/95 mL - water	1%/5 mL	20 nm
Frens [73]		0.2%/50 mL - water	1%/0.5 mL	16 nm
Yonezawa [74]		5.8×10^{-3} mol/25 mL - water	2.0%/25 mL	10 nm
Zhang [75]		0.01%/4 mL - water	1%/4 mL	10 nm
Mine [76]		0.24 mM/200 mL - water	0.34 M/0.94 mL	15 nm
Seitz [77]		0.5 M/40 mL - water	0.5 M/160 mL	40 nm
Yang [78]		24.3 mM/4 mL- ethanol	1.0 mM/100 mL	4 nm
Huang [79]		1 mM/500 mL - water	38.8 mM/50 mL	10 nm
Akiyama [80]		2.5×10^{-4} M/950 mL- water	38.8 mM/50 mL	18 nm
Grabar [81]	Variation 1	1 mM/500 mL- water	38.8 mM/50 mL	13 nm
	Variation 2	0.01%/500 mL - water	1%/7.5 mL	18 nm
Mayya [82]		240 mg/500 mL - water	1%/50 mL	12.6 nm
Storhoff [83]		1 mM/500 mL - water	38.8 mM/50 mL	13 nm
Ojea-Jiménez [84]	Variation 1	0.165 mM/149 mL - water	0.34 mM/1 mL	36.6 nm
			0.26 mM/1 mL	17.8 nm
	Variation 2	0.25 mM/149 mL - water	0.34 mM/1 mL	14.9 nm
			0.26 mM/1 mL	13.6 nm
Nirala [85]		1.0 mM/20 mL - water	1%/2 mL	15 nm
Mintz [86]		0.01%/50 mL - water	1%/2 mL	22.7 nm
Shi [87]		50 mL/1 mg/mL- water	2 mg/2 mL	13 nm
Takahashi [88]	Variation 1	a = 0.01%/100 mL - water use 4 mL from a	1%	15 nm
	Variation 2	use 1.5 mL from a	1%	25 nm
Sangamithirai [89]		5 mM/100 mL - water	125 mM/10 mL	5 nm
Li [90]		0.01%/30 mL - water	1%/200 mL	50 nm
Hanžić [91]		4%/102.5 μL - water	1%/848.4 μL	14 nm
Niu [92]		0.2 g/100 mL - water	10 g/4.0 mL	13 nm
Uthaman [93]		1 mM/50 mL - water	38.8 mM/5 mL	21.61 nm
Karakocak [94]		10 mg/90 mL - water	38.8 mM/5 mL	Best result 50 nm
			400 μL–900 μL	
Panday [95]		25 mM - water added every 30min for two cycles	2.18 mM	22, 105 and 186 nm
He [96]		1 mM/50 mL - water	38.8 mM/4 mL	11 nm
Hong [97]		50 mg/510 mL - water	45 mg	32 nm
			75 mg	28 nm
			90 mg	22 nm
			180 mg	17 nm
Karpel [98]		3×10^{-4} M/100 mL - water	0.17 M/706 mL	14.6 nm
Perera [99]		0.415 g/1000 mL - water	1%/100 mL	13 nm
Bartosewicz [100]		5 mM/57 mL - water	0.02 M/3 mL	11.5 nm
Wang [101]		1 mM/25 mL - water	38.8 mM/2.5 mL	15 nm
Nebu [102]		1 mM/25 mL - water	38.8 mM/2.5 mL	20 nm
Thambiraj [103]		1 mM/100 mL- water	1 wt%/5 mL	21.75 nm

* the values were presented in the same form that the authors presented.

boiling, rapid addition of 50 mL of 38.8 mM sodium citrate to the vortex of the solution and a color change from pale yellow to wine-red was taken place. Boiling was continued for 10 min; the heating mantle was removed, and stirring was continued after the solution was cooled down to room temperature yielding particles of 10 nm [79].

Akiyama et al. boiled under refluxed an aqueous solution of $HAuCl_4$ (2.5×10^{-4} M, 950 mL). 50 mL of 1% sodium citrate solution was added to the boiling solution. The mean diameter of the particles, analyzed by transmission electron microscopy, was 18 nm [80].

Grabar et al. described two examples in their work using the Turkevich method: Preparation I. In a 1 L round-bottom flask equipped with a condenser, 500 mL of 1 mM $HAuCl_4$ was brought to a rolling boil with vigorous stirring. Rapid addition of 50 mL of 38.8 mM sodium citrate to the vortex of the solution resulted in a color change from pale yellow to burgundy. Boiling was continued for 10 min; the heating mantle was then removed, and stirring was continued for an additional 15 min. After the solution reached room temperature, it was filtered with a membrane filter. The resulting solution indicated a particle size of 13 nm. Preparation 2. In a 1 L round-bottom flask equipped with a condenser, 500 mL of 0.01% $HAuCl_4$ was brought to a boil with vigorous stirring. To this solution was added 7.5 mL of 1% sodium citrate. The solution turned blue within 25 s; the final color change to red-violet occurred 70 s later. Boiling continued for an additional 10 min, the heating source was removed, and the colloid was stirred for another 15 min. TEM data indicated an average diameter of 18 nm [81].

Mayya et at dissolved 240 mg of chloroauric acid ($HAuCl_4$) in 500 mL of water and brought the solution to ebullition, after which a solution of 1% sodium citrate (50 mL) was added with continued boiling for 1 h. Particles had 12.6 nm [82].

Storhoff et al. presented the synthesis: an aqueous solution of $HAuCl_4$ (1 mM, 500 mL) was brought to a reflux while stirring, and then 50 mL of a 38.8 mM sodium citrate solution was added quickly, which resulted in a change in solution color from pale yellow to deep red. After the color change, the solution was refluxed for an additional 15 min, allowed to cool to room temperature, and subsequently filtered through a 0.45 μm nylon filter. Particles were measured up to 13 nm [83].

Ojea-Jiménez et al. [84] reported in a typical experiment, an aqueous solution of $HAuCl_4$ (0.165 or 0.25 mM) in H_2O (149 mL) was heated up to 100 °C for 15 min. The reducing reagent, SC-sodium citrate (either 0.34 or 0.26 mM, respectively) in H_2O (1 mL) was

then added (direct method). The same experiment was repeated by maintaining the amounts of reagents but changing the order of reagents addition: an aqueous solution of SC (149 mL) was heated to reflux during 15 min before $HAuCl_4$ was added (1 mL) (inverse method). All reactions were maintained at the boiling point for 5 min before cooling them down to room temperature. Particles fabricated by the direct method has 36.6 and 17.8 nm for 13.6 and 6.8 SC/$HAuCl_4$ ratios, respectively. The indirect method yielded particles with 9 and 14.9 nm for 13.6 and 6.8 SC/$HAuCl_4$ ratios, respectively.

Nirala et al. presented a modified Turkevich method. Two milliliters of trisodium citrate dehydrate (1%) was added to the boiling solution of 20 mL of $HAuCl_4$ (1.0 mM) under constant stirring. The solution is removed from the hot plate when the color changed from colorless to wine red. The solution was cooled and kept under refrigeration for further use. Average size of 15 nm [85].

The synthesis of AuNPs was carried out by dissolving 50 mL of a 0.01% (w/v – weight per volume equivalency) solution of chloroauric acid in deionized (DI) H_2O. Once boiling, 2 mL of 1% sodium citrate (w/v) was added under constant, vigorous stirring. The mixture was left boiling for 10 min, then moved to cool in the dark. The final product collected was diluted up to 50 mL and stored in the dark at 4 °C until further use. The AuNPs averaged 22.7 nm in size [86].

Under vigorous stirring, $HAuCl_4$ (50 mL, 1 mg/mL) was heated to boiling, and then a sodium citrate solution (2 mL, 1 mg/mL) was rapidly added to a boiled $HAuCl_4$ solution. In order to ensure complete reduction, the mixed solution was boiled for 30 min and further stirred for 15 min. After the solution changed from pale yellow to wine-red, the solution was cooled to room temperature gradually and filtered by a filter film (pore size: < 0.45 μm) to remove the impurities, and the filtrate was stored at 4 °C. The authors achieved 13 nm particles [87].

Takahashi et al. reported 15 nm and 25 nm of AuNPs synthesized by the citrate-mediated reduction of $HAuCl_4$ [30]. One hundred milliliters of 0.01% (w/v) $HAuCl_4$ was heated to boil. Then, 4 mL (for 15 nm AuNPs) or 1.5 mL (for 25 nm of AuNPs) of 1% sodium citrate was added to the boiling solution under vigorous stirring. The solution was kept on stirring until the color of the solution turned to wine red indicating the formation of AuNPs. After continued heating for about 5 min, the colloidal solution was cooled down to room temperature. And the products were stored at 4 °C for further use [88].

In a typical procedure, Sangamithirai et al. prepared a 100 mL of 5 mM $HAuCl_4$ aqueous solution in a round-bottom flask and the solution was heated to boil under constant stirring. Subsequently, 10 mL of 125 mM sodium citrate was added rapidly to the above solution. The reaction mixture was boiled for another 15 min during which the solution color was changed from pale yellow to deep red. The obtained solution was continuously stirred and cooled down to room temperature. Average particle size was ca. 5 nm [89].

Fifty nanometer AuNPs were achieved by Li et al. trough heating 30 mL of 0.01% $HAuCl_4$ solution under vigorous stirring until boiling. Then, 200 mL of 1% sodium citrate was added rapidly to the solution. The color of the mixture gradually changed to brick-red. The resulting solution was cooled to room temperature under mild stirring and stored at 4 °C in a dark beaker [90].

An aqueous solution with 102.5 μL of 4% $HAuCl_4$ was added to deionized water (10 mL), which was heated to boiling. Aqueous solution of 1% sodium citrate (848.4 μL) was then added to the boiling solution, at which point the solution turned from clear yellow to a deep wine red. After cooling, the ruby red gold colloidal solution was filtered through a 0.22 μm filter and stored at 4 °C. The final size achieved by Hanžić et al. was 14 nm [91].

Niu et al. reported a gold colloid solution with 13 nm particles. Fifty milliliters of 0.2 g of $HAuCl_4$ was brought to a rolling boil with vigorous stirring in a 100 mL round-bottom flask. The rapid addition of 4.0 mL of 10 g of sodium citrate to the vortex of the solution resulted in a color change from pale yellow to orange red. Boiling was continued for 15 min, the heating mantle was then removed, and stirring was continued until the solution reached room temperature [92].

Uthaman et al. reported the following: 50 mL of 1 mM of $HAuCl_4$ was mixed with distilled water and boiled at 100 °C. When the temperature reached 100 °C, 5 mL of (38.8 mM) sodium citrate was rapidly added to the gold salt solution, resulting in a color change from light yellow to dark red. After this color change, the solution was stirred for 15 min, slowly cooled to room temperature, and purified by centrifugation. The DLS measurement indicated average hydrodynamic diameter of 21.61 ± 12.32 nm [93].

Karakocak et al. synthesized AuNPs by using $HAuCl_4$ (10 mg) was dissolved in 90 mL of deionized (DI) water, and this solution was heated to boiling. Sodium citrate solution (250 mM) was added to the boiling solution in amounts ranging from 400 μL to 900 μL and stirred for 20–30 min until the solution became wine-red. The solution was then left undisturbed in the dark for 24 h at room temperature. Subsequently, Au NP solutions were centrifuged at 10,000 rpm for 20 min and suspended in DI water (deionized water). Nanoparticles size was 50 nm [94].

Two point 2 mM of sodium citrate solution was heated at 100 °C under high stirring condition, followed by injection of 25 mM gold chloride, resulting in solution turning pale red color, suggestive of formation of gold nuclei. The solution was maintained at 100 °C for 30 min and then stepped down to 90 °C for 45 min to prevent further formation of gold nuclei. Additional 25 mM gold chloride was added every 30 min for two cycles. To enhance gold deposition on the formed gold nuclei, 35% of the reactant solution was replaced with equal volume of 2.18 mM of sodium citrate, followed by further addition of 25 mM gold chloride. Care was taken to ensure that the solution temperature was constantly maintained at 90 °C throughout the synthesis. The process of dilution and addition of 25 mM gold chloride was repeated for a total of 16 cycles, where 22, 105 and 186 nm sized citrate capped particles were obtained in the 1st, 13th and 16th dilution cycle [95].

Approximately 11 nm diameter gold nanoparticles were synthesized by the citrate reduction of $HAuCl_4$ by He et al. Briefly, 50 mL of 1 mM $HAuCl_4$ solution was added into a flask that was connected with a condenser and heated to boil while stirring. When the solution started boiling, 4 mL of sodium citrate solution (38.8 mM) was added. The reaction was heated for extra 20 min after the color changed from colorlessness to burgundy red. The solution was cooled down to 25 °C under stirring, and then stored in a light resistant container at 4 °C. Ultrasonic treatment was required prior to use if a small amount of metal plating was observed on the bottom sides of the bottles [96].

AuNPs were synthesized by Hong et al. as follows: 50 mg $HAuCl_4$ dissolved in 10 mL MilliQ water was added to 500 mL MilliQ water and heated until boiling. For the synthesis of different AuNPs sizes, 45, 75, 90, or 180 mg of sodium citrate (Fisher Scientific) dissolved in 10 mL MilliQ water was added and the solution was boiled for another 15 min before cooling to room temperature, constant stirring was maintained throughout the synthesis. The diameters of resulting particles were 32, 28, 22, and 17 nm respectively for the different amounts of sodium citrate added [97].

Karpel et al. used 706 mL of 0.17 M sodium citrate adding to 100 mL of 3×10^{-4} M $HAuCl_4$ (1:4 M ratio of $HAuCl_4$ to citrate) dissolved in water under reflux. The solution was kept under strong stirring and under reflux for 20 min. This procedure yielded particles with a diameter of about 14.6 nm [98].

Citrate-reduced AuNPs were synthesized by Perera et al. The

amount of precursor used was 0.415 g of $HAuCl_4 \cdot 3H_2O$ dissolved in 1000 mL of double-distilled Nanopure water. Those solution were brought to boil, and then 100 mL of 1% sodium citrate was added. Finally, the reaction solutions were further boiled for 20 min while stirring. The average diameter was 13 nm [99].

The solutions of AuNPs were prepared following the classical citrate method yielding particles with 11.5 nm. In a typical procedure, a 3 mL sample of aqueous $HAuCl_4$ (5 mM) was added to a 250 mL flask containing 54 mL of water at room temperature. The solution was brought to a boil while stirring magnetically (400 rpm) and then 3 mL of 0.02 M sodium citrate solution was added at once. The reaction was run until the solution became red in color and its color remained unchanged for the next 5 min [100].

Wang et al. used a $HAuCl_4$ solution (25 mL, 1 mM) that was heated to slight boiling in a flask. Sodium citrate (2.5 mL, 38.8 mM) was gently added with strong and uniform stirring. After 30 min of reflux, the mixture was slowly cooled down to room temperature. Finally, the product was filtered through a 200 nm filter membrane and stored at 4 °C for subsequent use. The average size was 15 nm [101].

The AuNPs synthesized by the reduction of $HAuCl_4$ with sodium citrate by Nebu et al. About 25 mL $HAuCl_4$ (1 mM) was mixed with 2.5 mL sodium citrate (38.8 mM) with vigorous stirring (600 rpm) for 10 min. The mixture was boiled (100 °C) under stirring and then the hot plate was turned off. A color change was observed within 10 min and the stirring was continued for 20 min. The solution was stored at 4 °C for further use. Nanoparticles had diameter with ca. 20 nm [102].

One hundred milliliters of 1 mM of $HAuCl_4$ was prepared in water and heated until it begins to boil. To this solution, 5 mL of 1 wt% of trisodium citrate in aqueous medium was added into the reaction mixture. This reaction was continued until the solution turned to wine red. This color change appeared within 3 min due of the reduction of Au^{3+} to Au^0 and the reaction was completed within 5 min. After the completion of the reaction, the obtained AuNPs solution was centrifuged at 5000 rpm for 20 min and the solution was stored at 4 °C. The average size of the synthesized AuNPs was found to be 21.75 nm [103].

4.2. Synthesis with $NaBH_4$ with/without citrate

Search key words: sodium borohydride; nanoparticles; gold.

The addition of sodium borohydride ($NaBH_4$) to the Turkevich method was established in an attempt to simplify the synthesis, by eliminating the heating process. Table 2 presents the number of research articles published using the modified Turkevich thought the years.

Table 3 presents a summary of the papers presented.

In Kalimuthu et al., 1 mL of 1% $HAuCl_4$ was added to 90 mL of H_2O at room temperature. After 1 min of stirring, 2.00 mL of 38.8 mM sodium citrate was added. One minute later, 1.00 mL of fresh 0.075% $NaBH_4$ in 38.8 mM sodium citrate was added. The colloidal solution was stirred for an additional 5 min and stored in a dark bottle at 4 °C. Particles had 13 nm [104,113].

Table 2
Number of research articles published between 2003 and 2018 using the modified Turkevich.

Year	Papers
2003	2
2006	1
2010	1
2012	1
2013	1
2016	1
2017	2
2018	1

Zhao et al. reported: 50 mL sample of aqueous $HAuCl_4$ (0.25 mM) containing specific amounts of NaCl was put into a 100 mL flask cooled by ice water (4 °C) while magnetically stirring, and then 2 mL of 1% aqueous solution of sodium citrate was added after 1 min. After an additional 1 min, 0.5 mL of 0.25% aqueous solution of $NaBH_4$ containing 1% sodium citrate was added. Gold nanoparticles were obtained after the reaction solution was kept at 4 °C for 5 min. Particles presented 19 nm in size [105].

Wang et al. used an aqueous solution containing (0.1 mM, 100 mL) $HAuCl_4$ and 0.15 mM trisodium citrate was prepared (no info in volume was provided). Next, 1 mL of 0.05 M $NaBH_4$ solution was added at once into the gold solution under continuous stirring. Aqueous solution was then mixed and stirred vigorously for 2 h. Prepared Au colloid with 6 nm was stored in a dark glass bottle at 4 °C for further use [106].

Iqbal et al. described: 10 mg of $HAuCl_4$ was dissolved in 100 mL of deionized water (0.25 mM) and shaken properly to mix the solution. And, 0.1 M solution of reducing agent ($NaBH_4$) was prepared by dissolving 1.891 g of $NaBH_4$ in 500 mL of deionized water. Then, 100 mL of $HAuCl_4$ (0.25 mM) were taken in 250 mL flask with magnetic stirring at 750 rpm and the reducing agent solution was added drop by drop with continuous stirring. The color of $HAuCl_4$ solution changed from pale yellow to dark red over several minutes. Stirring process was continued for another 10 min for complete homogenization. After preparation of the particles, the dispersions were centrifuge at 14,000 rpm for 15 min and the collected particles were redispersed in deionized water. Characterization reveal particles with 30 nm [107].

Kesik et al. affirms that in order to have spherical AuNPs with 3.5 nm, a three-step synthesis procedure was carried out. Firstly, 9.5 mL ultra-pure deionized (DI) water, 0.25 mL (0.01 M) $HAuCl_4$, and 0.25 mL (0.01 M) Na-citrate were mixed homogeneously. Subsequently, 0.3 mL (0.1 M) freshly prepared, ice-cold $NaBH_4$ solution was added until pink color of the solution was observed. The solution was kept undisturbed at room temperature for 3 h to obtain spherical AuNPs (3.5 nm in diameter) [108].

In a typical experiment, Aryal et al. reduced 100 mL aqueous solution of $HAuCl_4$ (10^{-4} M) with 0.01 g of $NaBH_4$ at room temperature resulting in the formation of ruby-red gold hydrosol containing gold nanoparticles with diameter about 7 nm [109,114]. Average size was 7 nm.

Wang et al. reported 4 nm diameter of AuNPs were synthesized by reduction of $HAuCl_4$ with sodium borohydride in the presence of sodium citrate. Briefly, 645 μL of 1% sodium citrate was added to 100 mL of 0.01% (w/v) $HAuCl_4$ under vigorous stirring. After stirring at room temperature for 3 min, 3 mL of 0.1 M $NaBH_4$ which was freshly prepared in ice-cold water was added to the mixture, and the color of the solution changed quickly from colorless to red. After continued stirring for another 30 min, the formed colloidal solution was standing at room temperature for 2 h without stirring. Finally, the prepared 4 nm AuNPs were stored at 4 °C for further use [110].

In a typical synthesis, Shajkumar et al. added 107.4 mg (0.27 mM) of $HAuCl_4$ to a flask with deionized water. After 1 min, 11 mL of aqueous solution of tri-sodium citrate (1 wt%) was added. Another 30 s later, 5.5 mL of freshly prepared ice-cold aqueous solutions of sodium borohydride (0.08 wt%) and sodium citrate (1 wt%) were quickly injected. The resulting volume of the reaction mixture was 500 mL. After 10 min of stirring, solution was cooled down to room temperature. AuNP size after measurement was 7.5 ± 2.8 nm [111].

Chaudhary et al. used sodium borohydrate in their nanoparticle synthesis. Briefly, 100 mL of 1 mM aqueous solution of $HAuCl_4$ was

Table 3
Summary of the papers presented for the Synthesis with $NaBH_4$ with/without citrate.

Synthesis with $NaBH_4$ with/without citrate				
Reference	$HAuCl_4$ (concentration of $HAuCl_4$/volume - in water)	$NaBH_4$ (concentration in water or mass of $NaBH_4$ added)	Citrate (concentration in water or mass of citrate added)	AuNP size
Kalimuthu [104]	1%/1 mL	0.075%/1.00 mL $NaBH_4$ in 38.8 mM sodium citrate solution	38.8 mM/2.00 mL	13 nm
Zhao [105]	0.25 mM/50 mL	0.25%/0.5 mL $NaBH_4$ containing 1% sodium citrate	1%/2 mL	19 nm
Wang [106]	0.1 mM/100 mL	0.05 M/1 mL	0.15 mM	6 nm
Iqbal [107]	10 mg/100 mL	1.891 g/500 mL	Not used	30 nm
Kesik [108]	0.01 M/0.25 mL $HAuCl_4$	0.1 M/0.3 mL	0.01 M/0.25 mL	3.5 nm
Aryal [109]	10^{-4} M/100 mL	0.01 g of $NaBH_4$	Not used	7 nm
Wang [110]	0.01%w/100 mL	0.1 M/3 mL	1%/645 μL	4 nm
Shajkumar [111]	0.27 mM/500 mL	0.08 wt%/5.5 mL	1 wt%/5.5 mL	7.5 nm
Chaudhary [112]	1 mM/100 mL	100 mM/3 mL	38.8 mM/8 mL	24.5 nm

mixed with 8 mL of 38.8 mM aqueous sodium citrate solution. Three milliliters of 100 mM aqueous solution of ice-cold $NaBH_4$ was added dropwise under vigorous stirring and incubated for 24 h under constant stirring to decompose residual sodium borohydrate. A redish colloidal solution of gold nanoparticles was formed. The solution was centrifuged at 2500 rpm for 5 min. The final size was 24.5 nm [112].

4.3. Synthesis by Brust-Schiffrin method

Search key words 1: tetraoctylammonium bromide; nanoparticles; gold.

Search key words 2: dodecanethiol; nanoparticles; gold.

Search key words 3: Brust; nanoparticles; gold.

Fig. 8 presents the amount of published papers for the Brust-Schiffrin method.

One of the most well-known ways to synthesize spherical GNPs that are soluble in organic solvents is the Brust-Schiffrin method [46]. The formation of small nanoparticles (<10 nm in diameter) is due to the high affinity of the thiol ligands to gold surface, preventing NPs growth [46]. Table 4 presents a summary of the papers presented.

The method known as "Brust-Schiffrin" is as follows: An aqueous solution of $HAuCl_4$ (30 mL, 30 mM) was mixed with a solution of tetraoctylammonium bromide (TOAB) in toluene (80 mL, 50 mM). The two-phase mixture was vigorously stirred until all the tetrachloroaurate was transferred into the organic layer and dodecanethiol (170 mg) was then added to the organic phase. A freshly prepared aqueous solution of sodium borohydride (25 mL, 0.4 M) was slowly added with vigorous stirring. After further stirring for 3 h the organic phase was separated, evaporated to 10 mL in a rotary evaporator and mixed with 400 mL ethanol to remove excess thiol. The mixture was kept for 4 h at −18 °C and the dark brown precipitate was filtered off and washed with ethanol. The crude product was dissolved in 10 mL toluene and again precipitated with 400 mL ethanol. Particle produced by this method reached 2.5 nm [46,133].

Shon et al. presented: 0.39 g (1.0 mM) of $HAuCl_4$ was dissolved in 40 mL of nanopure H_2O and 1.09 g (2.0 mM) of TOAB in 160 mL of toluene was added to the reaction flask. The reaction mixture was stirred for 10 min before the addition of 0.38 g (10 mM) of $NaBH_4$. The resulting solution containing TOAB-AuNPs with 3.4 nm exhibiting a strong purple/red color [115].

The preparation technique of Praharaj et al. is as follows. To an aqueous solution of $HAuCl_4$ (1 mL, 10 mM), 20 mg of TOAB (tetraoctylammonium bromide) was added and toluene (20 mL) was introduced above the aqueous layer. Upon shaking, $AuCl_4^-$ ions were transferred from aqueous phase to the organic layer. The gold solution was divided in two vials containing different organic molecules CTAC (cetyltrimethylammonium chloride) and CTAB (cetyltrimethylammonium bromide). Each solution was mixed well so that the final concentration of stabilizers in all the sets was

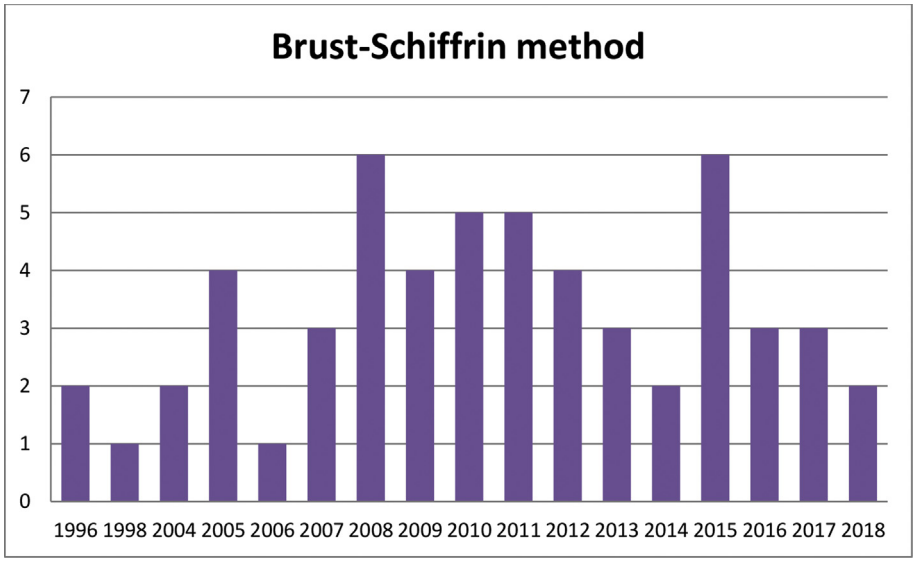

Fig. 8. Number of research articles published using Brust-Schiffrin between 1996 and 2018.

Table 4
Summary of the papers presented for the Brust-Schiffrin method.

Synthesis by Brust-Schiffrin method			
Reference	$HAuCl_4$ (concentration of $HAuCl_4$/volume)	Other chemicals used	AuNP size
Brust-Schiffrin [46]	30 mM/30 mL	• dodecanethiol- 170 mg • TOAB- 30 mM/80 mL • NaBH4 - 0,4 mM/25 mL	2.5 nm
Shon [115]	0.39 g	• TOAB- 1.09 g • NaBH4- 0.38 g	3.4 nm
Praharaj [116]	10 mM/1 mL	• TOAB- 20 mg • NaBH4 - 1 mg of sodium borohydride	10 nm
Briñas [117]	30 mM/30 mL	• Pentanethiol- 170 mg • TOAB- 50 mM/80 mL • NaBH4 - 0.4 M/25 mL	5 nm
Kuroda [118]	10 mM/60 mL	• mercaptopropionic acid- 30 mM/20 mL • TOAB- 7.5 mM/160 mL • NaBH4 - 6 mM/60 mL	3 nm
Ghosh [119]	30 mM/30 mL	• TOAB- 25 mM/80 mL • NaBH4 - 0.4 M/25 mL	20 nm
Quintana [120]	0.45 mM/15 mL	• dodecanethiol- 0.45 mM • TOAB- 1 mM/40 mL • NaBH4 - 5 mM/12 mL	1.8 nm
Vörös [121]	3.4×10^{-2} M	• TOAB- 3.4 × 10−2 M • NaBH4 - no information	1.8 nm
Zhang [122]	30 mM/80 mL	• TOAB- 25 mM/80 mL • NaBH4 - 0.4 M	5–15 nm
Liu [123]	310 mg/25 mL	• decanethiol- in excess 17 L • TOAB- 1.5 g/80 mL • NaBH4 - 0.38 g/25 mL	3.75 nm
Kang [124]	30 mM/30 mL	• TOAB- 25 mM/80 mL • NaBH4 - 0.4 M/25 mL	5.5 nm
Wang [125]	0.03 M/6 mL	• TOAB- 0.15 M/6 mL • NaBH4 - 0.26 M/6 mL	52 nm
Kim [126]	4.0 mM/120 mL	• chlorobenzenemethanethiol- 0.32 g/2.0 mM • TOAB- 5.5 g/240 mL • NaBH4 - 0.8 g/50 mL	3–4 nm
Kyrychenko [127]	A) 0.05 M $HAuCl_4$ in 1.0 M aqueous HCl 100 mL of A/10 mL	• dodecanethiol- 0.1 g in 5 g of n-hexane • NaBH4 - 0.05 M in 1.0 M/100 μL aqueous NaOH	3.75 nm
Du [128]	1) 20:1 M ratio of n-Dodecanethiol/$HAuCl_4$ into a 60 mL of 95% ethanol solution 2) 0.103 M/1.5 mL	• dodecanethiol • NaBH4 - 2%/2 mL	10 nm
Tianimoghadam [129]	0.03 M/3 mL	• dodecanethiol- 17 mg • TOAB- 0.05 M/8 mL • NaBH4 - 0.4 M/2.5 mL	3–4 nm
Lee [130]	300 mg/30 mL	• dodecanethiol- 2400 mL • TOAB- 2 g/80 mL • NaBH4 - 0.4 M/25 mL	5 nm
Dichello [131]	0.25 g/0.64 mM	• triphenylphosphine- 0.58 g • TOAB- 0.4 g • NaBH4 - 0.35 g/10 mL	2.8
Razzaq [132]	5.18×10^{-3} M/160 mL	• 1-hexanethiol- 0.016 M • TOAB- 0.02 M/160 mL • NaBH4 - 6.74 × 10−2 M/160 mL	2 nm

maintained to 5 mM. Finally, 1 mg of sodium borohydride was introduced to each solution and all the reaction mixtures were shaken vigorously. During shaking, at first, the yellow color due to $AuCl_4^-$ disappeared and the solution became colorless within a few minutes. The solution turned into wine red on further shaking. The final concentration of gold was 0.5 mM and particle size were 10 nm. The slower rate of photo discoloration in presence of chloride counter ions has been authenticated to higher electron affinity of chlorine than bromine and the higher stability constant of bromocomplex than the corresponding chlorocomplex [116].

Briñas et al. mixed a solution of aqueous $HAuCl_4$ (30 mM, 30 mL) with a toluene solution of tetraoctylammonium bromide (50 mM, 80 mL). Pentanethiol (170 mg, 0.84 mM) was then added, followed by the slow addition of $NaBH_4$ solution (0.4 M, 25 mL). The mixture was stirred for 10 min at room temperature. The organic layer was collected and concentrated by rotary evaporation to 10 mL. Ethanol (500 mL) was added, and the mixture was kept at 4 °C overnight. The precipitate, with 5 nm particles, was collected by centrifugation, redissolved in toluene, and reprecipitated by the addition of ethanol. After cooling the mixture at 4 °C, the dark brown precipitate was collected and dried under vacuum overnight [117].

Kuroda et al. presented a synthesis were MPA (3-mercaptopropionic acid) was used instead of alkanethiols. An aqueous solution containing 10 mM $HAuCl_4$ (60 mL) was mixed with a solution of 7.5 mM tetraoctylammonium bromide in toluene (160 mL) and stirred vigorously for 10 min. An aqueous solution containing 30 mM MPA (20 mL) was then added into the mixture followed by further stirring for 10 min. A freshly prepared aqueous solution containing 6 mM of sodium borohydride (60 mL) was immediately added to the mixture. The solution was stirred overnight. The aqueous phase of 2 nm AuMPA particles was collected. The carboxyl groups of MPA were deprotonated into carboxylate groups by sodium hydroxide produced by the decomposition of $NaBH_4$, which made AuMPA dispersed in water [118].

The gold nanoparticles were prepared from $HAuCl_4$ in aqueous

solution with a reducing agent, $NaBH_4$, and a stabilizer, DMAP (4-(N,*N*-dimethylaminopyridine)) by Ghosh et al. In a typical preparation, to an aqueous solution of $HAuCl_4$ (30 mM, 30 mL), a solution of tetraoctylammonium bromide in toluene (25 mM, 80 mL) was added as the phase transfer reagent. The addition of the phase transfer reagent to the aqueous phase resulted in swift movement of the $AuCl_4^-$ ions to the organic layer within a few seconds. Then, a 0.4 M aqueous solution of freshly prepared $NaBH_4$ (25 mL) was added to the biphasic solution and stirred well. Upon addition of the reducing agent, the "toluenic" solution changed color from light yellow to wine red within a few minutes. After 30 min, the two phases were separated and the toluene phase was subsequently washed with 0.1 M H_2SO_4, 0.1 M NaOH, and H_2O (three times) and then, dried over anhydrous Na_2SO_4. Then, solid 0.980 g of DMAP was added directly to the toluene phase to precipitate the particles. The precipitate was washed three times with toluene to remove the unreacted DMAP molecules. Finally, the precipitate was resuspended in water to have an aqueous dispersion of only DMAP-stabilized particles with 20 nm average size (free from unreacted DMAP) [119].

Quintana et al. provided their synthesis steps in detail. A 0.45 mM $HAuCl_4$ solution was dissolved in 15 mL of purified water and 1 mM of TOAB was dissolved in 40 mL of toluene. The two solutions were mixed and vigorously stirred. Then, the stabilizer (dodecanethiol, 0.45 mM) was added to the mixture and subsequently, $AuCl^{4-}$ was reduced by adding dropwise a solution of 5 mM of $NaBH_4$ in water (12 mL). The organic phase turned from orange to intense brown indicating the formation of gold nanoparticles. After about 30 min of further stirring the toluene phase was separated from the aqueous phase and concentrated up a volume of about 2 mL before to be diluted with 400 mL of ethanol. The solution presented particles with 1.8 nm was kept for at least 2 h at −22 °C and the precipitate was then filtered with 0.45 μm nylon membrane and washed with fresh ethanol [120].

Vörös et al. used 3.4×10^{-2} M TOAB in toluene and mixed with 3.4×10^{-2} M aqueous solution of $HAuCl_4$. The two-phase mixture was intensively stirred until the all amount of gold chloride was transferred into the organic phase by the surfactant. The organic phase was separated and thiol compounds were added into Au:thiol = 1:1 M ratio. This solution was again stirred for 10 min at room temperature, followed by addition of the reducing agent, the freshly prepared aqueous solution of $NaBH_4$. The organic phase was separated and evaporated in a vacuum evaporator. The concentrated gold solution with 1.8 nm average size was then washed with ethanol and dried [121].

Zhang et al. added a 30 mM aqueous metal chloride solution ($HAuCl_4$) to a 25 mM solution of TOAB in toluene (80 mL). Then a 0.4 M solution of freshly prepared $NaBH_4$ was added to the stirred mixture. After 30 min, the two phases were separated and the toluene phase was subsequently washed with 0.1 M H_2SO_4, 0.1 M NaOH, and H_2O (three times), and then dried over anhydrous $NaSO_4$. Particle size range from 5 to 15 nm [122].

Liu at. Al. presented in their paper a synthesis in which $HAuCl_4$ (310 mg, 1 equiv.) was dissolved in 25 mL nanopure water and phase transferred to 80 mL toluene using 1.5 g of tetraoctylammonium bromide. Following, 1-decanethiol (17 L, 1/11 equiv.) and aqueous solution of $NaBH_4$ (0.38 g, 10 equiv., in 25 mL nanopure water) were added into the organic phase, the reaction solution was stirred at room temperature for 3 h. Particles yielded 3.75 nm size [123].

Kang et al. used a 30 mM aqueous metal chloride solution ($HAuCl_4$, 30 mL) and added to a 25 mM solution of tetraoctylammonium bromide in toluene (80 mL). A 0.4 M solution of freshly prepared $NaBH_4$ (25 mL) was added to the stirred mixture, which caused an immediate reduction reaction to occur. After 30 min, the two phases were separated and the toluene phase was subsequently washed with 0.1 M H_2SO_4, followed by 0.1 M NaOH, and lastly H_2O, and then the toluene phase was dried over anhydrous $NaSO_4$, yielding the gold nanoparticles. An aqueous 0.1 M 4-dimethylaminopyridine (DMAP) solution (1 mL) was added to aliquots (1 mL) of the as-prepared nanoparticle mixtures. The 0.1 M concentration of the DMAP solution was found to be sufficient to cause complete and spontaneous phase transfer of the nanoparticles. Direct phase transfer across the organic/aqueous phase boundary was completed within 1 h, with no stirring or agitation. Solid DMAP was added directly to the toluene solution to precipitate the 5.5 nm particles, which could then be resuspended in water [124].

Wang et al. presented their synthesis. Briefly, an aqueous solution of $HAuCl_4$ (0.03 M, 6 mL) was added to a solution of TOAB in toluene (0.15 M, 6 mL). The yellow aqueous phase became colorless, and the toluene phase turned orange. After stirring for 10 min at room temperature, a freshly prepared aqueous solution of sodium borohydride, $NaBH_4$ (0.26 M, 6 mL), was added dropwise into the reaction mixture over a period of 30 min, after which the mixture was vigorously stirred for additional 30 min. Subsequently, the organic phase was separated and was washed with 1% H_2SO_4 once and then with nanopure water five times. Finally the organic phase was dried using $MgSO_4$ and filtered through a filter paper resulting in 52 nm particles [125].

Kim et al. added 120 mL of $HAuCl_4$ solution (1.6 g, 4.0 mM) to TOAB (5.5 g, 10.0 mM) dissolved in toluene (240 mL) and stirred for 2 min. Chlorobenzenemethanethiol (0.32 g, 2.0 mM) dissolved in toluene was added followed by sodium borohydride (0.8 g) in water (50 mL). The mixture solution was stirred for 3 h, the toluene phase was separated and solution volume was reduced to 30 mL. The crude product was precipitated into methanol (500 mL), and then filtered and washed with methanol (400 mL). Final particle size was between 3 and 4 nm [126].

Kyrychenko et al. presented a multi-step synthesis. On the first step, starting solutions were prepared with deionized water: 0.05 M of $HAuCl_4$ in 1.0 M aqueous HCl (A), 0.05 M of $NaBH_4$ in 1.0 M aqueous NaOH (B) and 0.1 g of dodecanethiol in 5 g of n-hexane (C). One hundred microliters of solution A was added to 10 mL of deionized water under intensive stirring (with magnet stirrer) resulting in formation of brightly-yellowish transparent mixture. Then 100 μL of solution B was added slowly, during this step the solution color turns to the intensively-red. After this, 5 g of acetone was added and the mixture was shaken manually several seconds. Then solution C was added rapidly and the mixture was shaken manually during 30 s. Finally, the mixture was left quiet to allow the water and hexane layers to separate well one from another. The decolorization of the lower water phase was observed with the simultaneous dyeing of the upper organic phase. After that, the layer of n-hexane was removed. The procedure was repeated 10 times; all the collected n-hexane layers were combined together and concentrated in vacuum rotary evaporator under mild warming. The resulting concentrated solution was mixed with 5 mL of ethyl alcohol, from which the AuNPs were precipitated as dark amorphous solid. The precipitate was again dissolved in n-hexane and re-precipitated by ethanol to complete removing of dodecanethiol. The synthesized AuNPs were stable in solid state and in solutions in the non-polar solvents. The prepared AuNPs, with 3.75 nm, were stored at 4–5 °C [127].

Du et al. used 20:1 M ratio of n-Dodecanethiol/$HAuCl_4$ to synthetize gold nanoparticles. This solution was first added into a 60 mL of 95% ethanol solution, and then 2 mL of 2% sodium borohydride was added and stirred for 10 min. After that 1.5 mL of 0.103 M $HAuCl_4$ solution was added and further stirred for 30 min. In the beginning 5 min, the solution turned purple, following with

pale red later. Particles were pentagonal with 10 nm [128].

Tianimoghadam et al. used a solution of TOAB in toluene (8 mL, 0.05 M) and mixed with a yellow aqueous solution of $HAuCl_4$ (3 mL, 0.03 M). The two-phase mixture was vigorously stirred for 3 h until all the $AuCl_4^-$ was quantitatively transferred to the organic phase from the aqueous phase by complexation with the cationic part of TOAB. Stirring was continued until the orange-tinted aqueous phase turned colorless, confirming successful transfer of Au^{3+} into the organic layer on top. Dodecanethiol (17 mg) was then added to the organic phase. A freshly prepared aqueous solution of $NaBH_4$ (2.5 mL, 0.4 M) was then slowly added with vigorous stirring. An instant color change occurred in the organic phase from orange to black/brown and, ultimately, to dark purple. After further stirring for 3 h, the organic phase was separated and mixed with ethanol to remove excess thiol. The mixture was cooled for 4 h at −18 °C, and the dark brown precipitate was filtered off and washed with ethanol. The crude product was dissolved in 5 mL of toluene and again precipitated with excess ethanol. The result were 3–4 nm particles [129].

To prepare dodecanethiol-coated AuNPs, $HAuCl_4$ (300 mg) dissolved in deionized water (30 mL) was vigorously mixed with tetraoctylammonium bromide (2 g) dissolved in toluene (80 mL) for 2 h. After removing the water phase, 25 mL of aqueous sodium borohydride (0.4 M) was slowly added to the organic phase (toluene). After stirring the solution for 24 h, the organic phase was extracted and washed using first 0.1 M sulfuric acid and then deionized water. The solution was mixed with excess dodecanethiol (2400 mL) for 2 h. The toluene in the solution was evaporated, resulting in the production of a dried powder. The obtained powder was dispersed in chloroform and ultracentrifuged at 25,000 rpm for 600 s to separate the AuNPs from the unreacted chemicals. Next, the dried precipitates were again dissolved in chloroform (10 mg/mL), and then stored at 4 °C. The final AuNPs had 5 nm in diameter [130].

Dichello dissolved $HAuCl_4$ (0.25 g, 0.64 mM) and TOAB (0.4 g, 0.73 mM) in nitrogen sparged water/toluene (13 mL/17 mL) followed by addition of triphenylphosphine (0.58 g, 2.21 mM) under vigorous stirring. Freshly prepared aqueous sodium borohydride (0.35 g, 9.4 mM, dissolved in 10 mL) was then added at once by injecting directly into the organic phase, triggering a color change to dark purple. The resulting mixture was stirred for 3 h under a nitrogen atmosphere before the organic phase was isolated and washed tree times with distilled water. The product was further washed with a series of hexane and methanol:water (2:3) to remove the phase-transfer catalyst and unreacted starting materials. Characterization revealed an average gold core size of 2.8 ± 1.2 nm [131].

A solution of $HAuCl_4 \cdot 3H_2O$ in Milli-Q water (5.18×10^{-3} M, 160 mL) was added to a toluene solution of TOAB (0.02 M, 160 mL) with vigorous stirring. After 40 min, the water phase was discarded and 1-hexanethiol (0.016 M) was added to the organic phase. The reaction between Au (III) and the thiol was allowed to proceed. A freshly prepared aqueous solution of $NaBH_4$ (6.74×10^{-2} M, 160 mL, 1:13 M ratio of Au:$NaBH_4$) was then rapidly added to the mixture at 0 °C with vigorous stirring. The solution turned black immediately and the reaction mixture was left with stirring for 15–30 min for the different preparative conditions tested. The phases were separated, the organic phase extensively cleaned with water and then toluene removed by rotatory-evaporation ($T \leq 30$ °C). The black residue was re-suspended in absolute ethanol (160 mL), sonicated and left to settle overnight. The solution was then filtered through a sintered disc filter funnel and the filtrate transferred to a round-bottomed flask to remove the ethanol under vacuum. The nanoparticles were then suspended in approximately 160 mL of acetonitrile, sonicated for 15 min and left standing overnight. Finally, the particles were filtered and washed with acetonitrile. A size smaller than 2 nm was found by Razzaq et al. [132].

4.4. Synthesis by Seeding- Growth method

Search key words: seeding; nanoparticles; gold.

Search key words 2: seed mediated; nanoparticles; gold.

Fig. 9 presents the amount of published papers for the Seeding-Growth method.

In the seeded-growth method a reducing agent is used to form in a first stage Au(0) nanoseeds from a gold precursor. These seeds are induced to grow into gold nanorods in a second stage by using molecules (usually cationic surfactants) that adsorb preferentially on specific crystal facets showing high surface energies. Often, small concentrations of additional ions (such as or halides) are used as surface passivation components in a structure-directing role that enables control on the nanorod aspect ratio [134]. Table 5 presents a summary of the papers presented.

Jana et al. describes in detail how to perform the seeding-growth procedure. A majority of papers use this procedure with minor changes.

For preparing AuNPs, 20 mL aqueous solution containing 2.5×10^{-4} M $HAuCl_4$ and 2.5×10^{-4} M trisodium citrate was prepared in a conical flask. Next, 0.6 mL of ice-cold, freshly prepared 0.1 M $NaBH_4$ solution was added to the solution while stirring. The solution turned pink immediately after adding $NaBH_4$, indicating particle formation. The particles in this solution were used as seeds within 2–5 h after preparation. Here, citrate serves only as a capping agent since it cannot reduce the gold salt at room temperature (25 °C) [135].

For the growth solution, 200 mL aqueous solution of 2.5×10^{-4} M of $HAuCl_4$ was prepared in a conical flask. Next, 6 g of solid cetyltrimethylammonium bromide (CTAB- 0.08 M final concentration) was added to the solution, and the mixture was heated until the solution turned a clear orange color. The solution was cooled to room temperature and used as a stock growth solution [135].

Four sets of 50 mL conical flasks were labeled A, B, C, and D. In set A, 7.5 mL of growth solution was mixed with 0.05 mL of freshly prepared 0.1 M ascorbic acid solution. Next, 2.5 mL of seed solution was added while stirring. Stirring continued for 10 min after the solution turned wine red. Particles prepared this way were spherical with a diameter of 5.5 nm. Similarly, 9 mL of growth solution and 0.05 mL of 0.1 M ascorbic acid solution were mixed as set B, and 1.0 mL of seed solution was added while vigorously stirring. Stirring continued for 10 min. The solution's final color was deep red. Particles prepared this way were spherical with a diameter of 8.0 nm. The particles prepared here were used as seeds in set C 30 min after preparation. In set C, 9 mL of growth solution was mixed with 0.05 mL of 0.1 M ascorbic acid solution, and 1.0 mL from set B was added while stirring vigorously. Stirring was continued for 10 min. The final color of the solution was reddish brown. Particles prepared in this way were roughly spherical with a diameter of 17 nm. This solution was used as seed in set D 30 min after preparation. In set D, 9 mL of growth solution was mixed with 0.05 mL of 0.1 M ascorbic acid solution, and 1.0 mL from set C was added while stirring vigorously. Stirring continued for the next 10 min, and the final color of the solution was brown. Particles prepared this way consisted of a mixture of spheres (37 nm diameter) and rods (with an average major axis of 200 nm and minor axis of 17 nm). The solutions A, B, C, and D were stable for more than a month due the presence of CTAB as a particle stabilizer. Each solution, A-D, contained 2.5×10^{-4} M gold (atoms) [135]. Fig. 10 present a summary of this method.

Meng et al. presented: 0.05 mL, 50 mM $HAuCl_4$ was mixed with

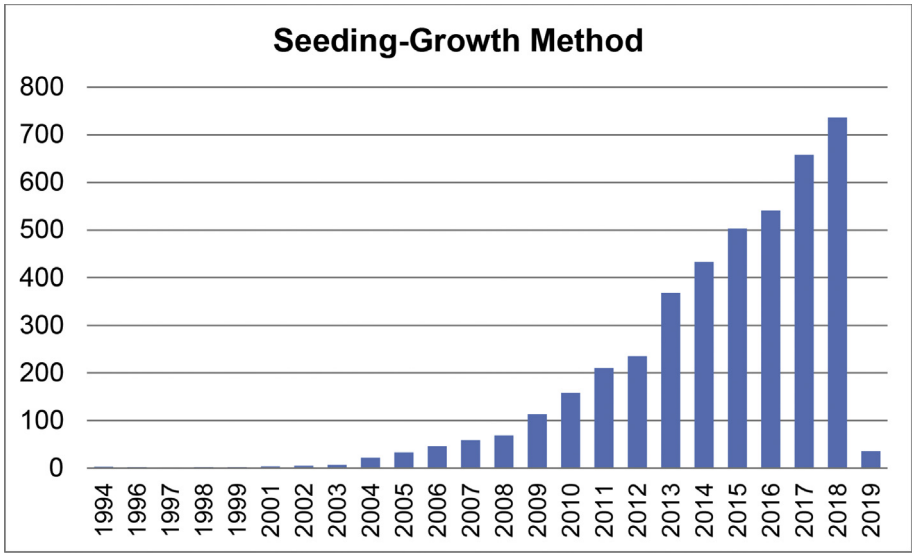

Fig. 9. Number of research articles published using the Seeding- Growth between 1994 and 2019.

Table 5
Summary of the papers presented for Seeding Growth.

Synthesis by Seeding Growth			
Reference	Seed Solution	Growth Solution	AuNP size
Jana [135]	• 20 mL- 2.5×10^{-4} M $HAuCl_4$ and 2.5×10^{-4} M trisodium citrate • $NaBH_4$ - 0.1 M/0.6 mL	• 200 mL aqueous solution- 2.5×10^{-4} M $HAuCl_4$ with 6 g CTAB[a]	5.5–37 nm
Meng [136]	• $HAuCl_4$- 50 mM/0.05 mL • CTAB- 0.1 M/10 mL • $NaBH_4$ - 10 mM/0.60 mL	• $HAuCl_4$- 50 mM/1 mL • CTAB- 0.10 M/1.0 mL • $AgNO_3$- 0.008 M • HNO_3- 2.0 M/1.0 mL • ascorbic acid- 0.1 M/0.6 mL	86 nm
Sahoo [137]	• $AgNO_3$- 0.1 mM/0.02 mL • ascorbic acid- 0.1 M/0.1 mL	• $HAuCl_4$- 0.25 mM • CTAB- 0.1 M • acetone- 0.2 mL • cyclohexane- 0.32 mL	10 nm
Spadavecchia [138]	• $NaBH_4$ - 0.01 M/0.6 mL • CTAB- 0.20 M/5 mL	• $HAuCl_4$- 1mM/5 mL • CTAB- 0.20 M/5 mL • $AgNO_3$- 4mM/0.25 mL • ascorbic acid- 8 mM/70 μL	3–32.6 nm
He [96]	• $HAuCl_4$- 2.5×10^{-4} M (2 mg) • $NaBH_4$ - 0.1 M/0.6 mL • sodium citrate 2.5×10^{-4} M (1.5 mg)	• $HAuCl_4$- 5 mg • 1,2-Bis(10,12-tricosadiynoyl)-*sn*-glycero-3-phosphocholine- 46 mg	1.5–30 nm
Wang [110]	• $HAuCl_4$- 0.01%w/100 mL • sodium citrate: 1%	• $HAuCl_4$- 0.01% w/100 mL • sodium citrate 1%w/220 μL hydroquinone 30 mM/1 mL	15–40 nm
Pan [139]	• $HAuCl_4$- 2.3×10^{-2} M/1 mL • trisodium citrate- 1.4×10^{-2} M/10 mL	• $HAuCl_4$- 2.3 mM/24 mL	18–60 nm
Nayef [140]	• $HAuCl_4$- 0.015 mM/50 mL • sodium citrate- 0.1 M/20 mL $NaBH_4$ - 0.01 M/0.6 mL	• $HAuCl_4$- 0.05 mM/200 mL • CTAB- 0.1mM/40 mL • ascorbic acid- 0.1 M/0.5 mL	31.41 nm

[a] Cetyl trimethyl ammonium bromide.

10 mL, 0.1 M CTAB solution at 27 °C Next, 0.60 mL of ice-cold 10 mM $NaBH_4$ solution was added quickly into the solution, which resulted in the formation of a brownish yellow solution. Vigorous stirring of the seed solution was continued for 2 min and was kept at 27 °C. Growth solution was prepared by adding CTAB (100 mL, 0.10 M) to 1.0 mL, 0.008 M $AgNO_3$ solution at 27 °C. Then 1 mL, 50 mM $HAuCl_4$ and 1.0 mL, 2.0 M HNO_3 was injected, followed by the addition of 0.6 mL, 0.1 M L of ascorbic acid. The color of growth solution was changed from dark yellow to colorless. Finally, 12 mL of gold seeds was injected into the growth solution at 28 °C. The nanorods with an aspect ratio of 2.8 were obtained. They presented 86 nm in length [136].

Sahoo et al. prepared in a 50 mL conical flask, 20 mL of growth solution containing 0.25 mM $HAuCl_4$, 0.1 M cetyltrimethyl ammonium bromide (CTAB), 0.2 mL acetone, and 0.32 mL cyclohexane. Then, 0.02 mL of 0.1 mM silver nitrate ($AgNO_3$) and 0.1 mL of 0.1 M freshly prepared ascorbic acid were added to the above growth solution with constant stirring. The orange color of gold salt in the growth solution disappeared after the addition of ascorbic acid and this change of color was due to the reduction of Au^{3+} to Au^{+}. Then, the growth solution was divided into four parts in four different 25 mL stopper conical flask containing 5 mL growth solution each. They were labeled as B, C, D and E. One milliliter of the seed solution (sample A) was added to the growth solution labeled B (step 1).

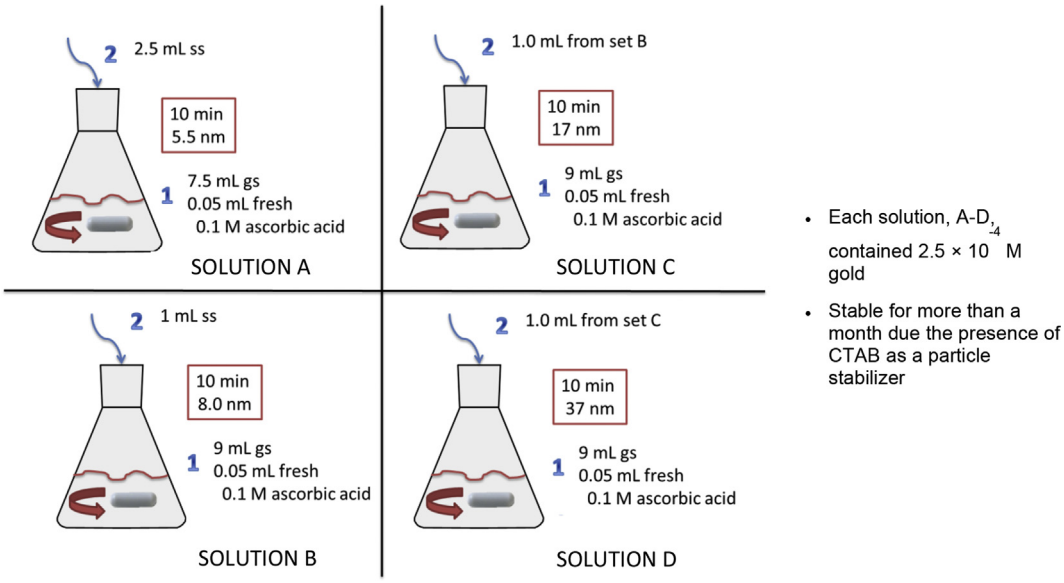

Fig. 10. Scheme for Jana et al. seeding growth method. (Caption: gs – Growth Solution; ss – Seeding Solution).

Rapid development of red color in sample B indicates the reduction of Au^{+} to Au^{0}. After 30 s, 1.0 mL of sample B was added to the growth solution C (step 2). Solution labeled sample C turns violet in color indicating the formation of anisotropic gold nanoparticles. Again, after 30 s, 1.0 mL of sample C was added to sample D (step 3). In the last step (step 4), 1.0 mL of sample D was added to sample E. Sample E became blue in color and it was due to the formation of highly anisotropic gold nanoparticles. Each solution of gold hydrosol was centrifuged for 10 min at a speed of 8000 rpm to precipitate out the particles from the solution and then re-dispersed in 5 mL doubly distilled water by sonication. Average particle size was 10 nm [137].

Spadavecchia et al. produced gold particles of around 3–4 nm, by using Au^{4+} ions and ice-cooled $NaBH_4$ (0.01 M; 0.6 mL) in the presence of CTAB (0.20 M; 5 mL). After 4 h, a calculated amount of this solution, was added to a growth solution containing CTAB (5 mL; 0.20 M), $HAuCl_4$ (5 mL; 1×10^{-3}), $AgNO_3$ (0.25 mL; 4×10^{-3} M) and ascorbic acid (70 μL; 8×10^{-3} M). The resultant solution was kept in dark for 24 h, deposited on a grid and examined by TEM. The as-prepared nanorod solution was centrifuged at 11,000 rpm for 26 min for three times and then the supernatant was discarded and the residue was redispersed in an equivalent amount of buffer solution (PBS, pH 7). The particles was shape as a rod with 32.6 nm in length and 13 nm width [138].

Guo et al. reported a synthesis using 100 mL of growth solution containing 0.5 mM $HAuCl_4$ and 0.1 M CTAB. To this solution 1 mL of 10 mM $AgNO_3$, 2 mL of 1.0 M HCl and 0.8 mL of 0.1 M L-ascorbic acid were added under gentle stirring. The orange color of the gold salt in the CTAB solution disappeared when ascorbic acid was added, due to the reduction of Au^{3+} to Au^{+}. The growth initiated by adding 0.8 mL of the seed solution to the growth solution. After the addition, the color of the growth solution changed from clear to violet red. The mixture solution was kept at 30 °C in water bath and left undisturbed overnight yielding 5 nm particles [141].

He et al. used 1,2-Bis(10,12-tricosadiynoyl)-*sn*-glycero-3-phosphocholine (PL) in their synthesis. *Preparation of seed solution:* 20 mL aqueous solution containing 2.5×10^{-4} M $HAuCl_4$ (2 mg) and 2.5×10^{-4} M trisodium citrate (1.5 mg) was prepared in a conical flask. Then, the ice-cold, freshly prepared 0.1 M $NaBH_4$ (0.6 mL, 2.3 mg) was added into the solution under stirring. The solution turned pink immediately after the addition of $NaBH_4$, indicating particle formation. The particles in this solution presented 1.5 nm and it was used within 2–5 h after preparation. *Preparation of growth solution:* 50 mL aqueous solution of 2.5×10^{-4} M $HAuCl_4$ (5 mg) was prepared in a conical flask. Then, 46 mg solid PL (0.001 M final concentration) was added into the solution and the mixture was heated until it became a purple color. Finally, the solution was cooled to room temperature and used as a stock growth solution. After the previous set up, sets A, B, and C containing 25 mL were prepared in a conical flask. In set A, 7.5 mL growth solution was mixed with freshly prepared 0.1 M ascorbic acid solution (0.05 mL, 1 mg). Then, 2.5 mL seed solution was added under stirring. Stirring continued for 10 min after the solution turned reddish purple. Particles prepared by this way were spherical with a diameter of 10 nm. Similarly, 9 mL growth solution and 0.1 M ascorbic acid solution (0.05 mL, 1 mg) were mixed as set B, and 1.0 mL seed solution was added under vigorously stirring. Stirring continued for 10 min. The solution's final color was ruby purple. Particles prepared by this way were spherical with a diameter of 17 nm. The particles prepared here were used as seeds in set C. In set C, 9 mL growth solution was mixed with 0.1 M ascorbic acid solution (0.05 mL, 1 mg), and then 1.0 mL solution from set B was added under stirring vigorously. Stirring was continued for 10 min. The final color of the solution was deep purple. Particles prepared by this way were roughly spherical with a diameter of 30 nm [96].

Wang et al. reported 15 nm and 25 nm of AuNPs were synthesized by the citrate-mediated reduction of $HAuCl_4$ [30]. Briefly, 100 mL of 0.01% (w/v) $HAuCl_4$ was heated to boil. Then, 4 mL (for 15 nm AuNPs) or 1.5 mL (for 25 nm of AuNPs) of 1% sodium citrate was added to the boiling solution under vigorous stirring. The solution was kept on stirring until the color of the solution turned to wine red indicating the formation of AuNPs. After continued heating for about 5 min, the colloidal solution was cooled down to room temperature. And the products were stored at 4 °C for further use. Those 15 nm AuNPs were used as seed particles for the synthesis of 40 nm AuNPs. Briefly, 3 mL of preformed 15 nm AuNPs and 220 μL of 1% sodium citrate were mixed with 100 mL of 0.01% (w/v) $HAuCl_4$. Then, 1 mL of 30 mM hydroquinone was added into the mixture quickly under vigorous stirring. The color of the solution

changed from light pink to wine red within 1 min. After continued stirring at room temperature for 10 min, the formed 40 nm AuNPs were stored at 4 °C [110].

For the seed nanoparticle fabrication, 1 mL of 2.3×10^{-2} M $HAuCl_4$ was mixed with 99 mL of DI H_2O, and then the mixture was heated to 110 °C for 5 min 10 mL of 1.4×10^{-2} M trisodium citrate was rapidly injected to the boiling solution. The mixture was stirred vigorously and refluxed for 20 min. The color of the mixture gradually changed after 5 min from a colorless to a pale red followed by pale purple and finally to a red wine color. After the color change process was completed, the colloidal solution was continuously stirred at room temperature for another 15 min until the solution cooled down. The size of the GNPs made by this method was approximately 18 nm. Larger sized GNPs (60 nm) were made based on the seed mediated growth method. Typically, for the fabrication of 60 nm GNPs, 10 mL of the seed GNP solution was diluted to 120 mL with the final trisodium citrate concentration of 3.7×10^{-3} M. The mixture was then heated to 110 °C and followed by gradually adding of 24 mL of 2.3×10^{-3} M $HAuCl_4$ to the hot solution. After the reaction was completed (approximately 25 min), the solution was gradually cooled down to room temperature and stored at 4 °C before usage [139].

AuNPs is synthesized by the seed-growth method by Nayef et al. Sodium citrate, 20 mL of 0.1 M, was mixed with $HAuCl_4$ (50 mL of 0.015 mM). Then 0.6 mL of ice-cold 0.01 M $NaBH_4$ was added to the mixture. Stirring continued for 5 min, the solution was kept at room temperature for 1 h (seeding solution). The growth solution was prepared by mixing 200 mL of 0.05 mM chloroauric acid with 40 mL of 0.1 mM CTAB, then adding 0.5 mL of 0.1 M Ascorbic Acid to this mixture. Five different experiments were prepared by adding different amounts of seed solution (1, 3, and 10 mL) to the 40 mL of growth solution. The sizes achieved were: 31.41, 32.38, and 47.86 nm, respectively [140].

4.5. Synthesis by ascorbic acid

Search key words: ascorbic acid; nanoparticles; gold.

Ascorbic acid (Vitamin C) is best known for its antioxidant role in biochemical reactions. It is environment friendly and possesses biodegradability, biocompatibility, low toxicity and high-water solubility. Different opinions exist in the literature regarding the ascorbic acid reduction capabilities: $HAuCl_4$ to $AuCl^{2+}$ or $HAuCl_4$ to Au^0. Table 6 presents a summary of the papers presented. Fig. 11 presents the amount of published papers for the Ascorbic Acid method.

Khan et al. stated that the reaction by mixing $[HAuCl_4] = 5.0 \times 10^{-5}$ M, [ascorbic acid] $= 8.0 \times 10^{-4}$ M and [CTAB] $= 5.0 \times 10^{-4}$ M. The solution became yellowish-turbid with a visible precipitate in the solution due to the complexation and/or solubility problem of CTAB and $HAuCl_4$. In the first set of experiments, a solution of ascorbic acid (4.0 mL 0.01 M) was added to a series of reaction mixtures containing $HAuCl_4$ (4.0 mL, 0.001 M) and CTAB (from 1.0 to 8.0 mL, 0.01 M, total vol. 20 mL) at 25 °C. It was observed that yellow colored reaction mixture became purple after the addition of ascorbic acid. In the second set of experiments, $HAuCl_4$ ($\geq 3.0 \times 10^{-4}$ M), a purple colored reaction was formed in ascorbic acid ($\geq 10.0 \times 10^{-4}$ M) and CTAB (20.0×10^{-4} M). Particles were irregular shaped with sizes from 24 to 42 nm [142].

Firdhouse et al. presented: 10 mL of 20 mM $HAuCl_4$ was added to 10 mL of 10 mM CTAB and 5 mL of 25 mM of ascorbic acid, and then incubated for 5 h at 37 °C. In the next step, the synthesized gold nanoparticles were centrifuged at 10,000 rpm for 15 min, and then washed three times by distilled water. The cubic particles, visualized by scanning electron microscopy, presented 15 nm [148]. Polyhedral gold nanoparticles like cubes, tetrahedrons, and octahedrons exhibit high index facets have increasing attention due to its applications in catalysis, plasmonic and SERS based sensors [143].

Chitosan-coated gold nanoparticles were synthesized by Boca et al. using ascorbic acid to reduce the gold salt and chitosan biopolymer to cap and stabilize the particles. First, 10 mL of 0.5×10^{-3} M of $HAuCl_4$ solution was stirred at room temperature for 5 min. Then, 1 mL of a freshly prepared solution of ascorbic acid (7.5×10^{-3} M) was added. The mixture rapidly turned colorless, dark blue and finally pinkish-red, demonstrating the formation of the particles with 18 nm. One milliliter of 2 mg/mL chitosan in 1% acetic acid solution (pH = 3) was added while continuing the stirring process for another 15 min [144].

In order to reduce Au^{3+} to Au^+, Biswal et al. added 7.2×10^{-4} M ascorbic acid to yellow colored aqueous solution containing 4×10^{-4} M of Au^{3+}, 0.1 M CTAB, 0.2 M of 2-propanol and 6×10^{-5} M Ag^+. After addition of ascorbic acid, the solution turned colorless, which indicates reduction of gold. The above solution containing AuI was subjected to gamma irradiation at a dose rate 3.4 kGy/h. As soon as the reaction medium was exposed to gamma radiation, the reduction of Au^+ to Au^0 took place by transient species generated from water radiolysis. The seed particle size was controlled by the high concentration of capping agent CTAB, which does not allow the seed to grow beyond a particular size. The irradiated solution was kept undisturbed for 2 h for subsequent growth of gold nanoparticles. The nanorods were 40 nm in length [145].

Lee et al. dissolved $HAuCl_4$ (0.05 M) and PVP-polyvinylpyrrolidone (weight ratio of PVP/$HAuCl_4$ = 1.1) in distilled water (1 mL each). Aqueous solution dissolving ascorbic acid (0.0375 M) was preheated up to 60 °C in a water bath. Then, 0.03 mL each of $HAuCl_4$ and PVP starting solutions was added in the

Table 6
Summary of the papers presented using Ascorbic Acid.

Synthesis by Ascorbic Acid			
Reference	Precursors	Ascorbic Acid -AA (concentration of AA/volume)	AuNP size
Khan [142]	• $HAuCl_4$- 1mM/4.0 mL • CTAB- 0.01 M/from 1.0 to 8.0 cm^3 mL	• AA- 0,01 M/4 mL	24–42 nm
Firdhouse [143]	• $HAuCl_4$- 20 mM/10 mL • CTAB- 10 mM/10 mL	• AA- 25 mM/5 mL	15 nm
Boca [144]	• $HAuCl_4$- 0.5 mM/10 mL	• AA- 7.5 mM/1 mL	18 nm
Biswal [145]	• $HAuCl_4$- 4×10^{-4} M • CTAB- 0.1 M • 2-propanol- 0.2 M • Ag^+ - 6×10^{-5} M	• AA- 7.2×10^{-4} M	40 nm
Lee [146]	• $HAuCl_4$- 0.05 M • PVP-polyvinylpyrrolidone (weight ratio of PVP/$HAuCl_4$ = 1.1)	• AA- 0.0375 M	65–95 nm
Patel [147]	• $HAuCl_4$- 10^{-2} M/200 mL	• AA- 20 mM	45 nm

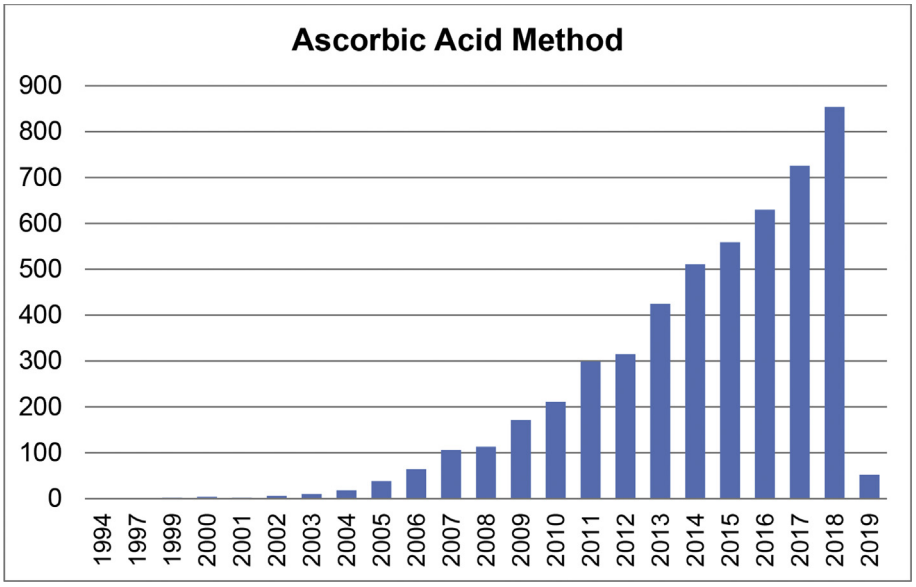

Fig. 11. Number of research articles published using Ascorbic Acid between 1994 and 2019.

preheated ascorbic acid solution to generate gold seeds. After 3 min, the residual starting solutions were added continuously in a dropwise manner at 0.06 mL/min. Sodium hydroxide (0.05 M) was added in the reacting solution after 5 min. The reacting solution was aged and vigorously stirred for 20 min at 60 °C. Centrifugation was undertaken to separate supernatant and product at 12,000 rpm for 30 min. The product was washed with distilled water and ethanol several times. Finally, the product was redispersed in ethanol for further characterization. Particles was polyhedral with 65–95 nm [146].

In a typical synthesis procedure by Patel et al., 10^{-2} M gold salt (200 mL) was mixed with 20 mM ice cold ascorbic acid (70 mL) under continuous stirring. The temperature of the reaction synthesis was maintained 4 °C throughout. With addition of gold salt, the colorless solution of ascorbic acid is changed to purple and finally faint blue. The average size of nanoflowers was measured to be of the order of 45 nm, the core size is around 35 nm, and length of the petals is around 5 nm [147].

4.6. Green synthesis methods

Search key words: green; nanoparticles; gold.

Synthesis of gold nanoparticles using plant extracts is well documented in the literature. Different composition and quantities of reducing agents are found in organic extracts influencing the final product. Various geometrical shapes and different sizes may be obtained impacting function and thus use. Different plants amino acids, enzymes, flavonoids, aldehydes, ketones, amines, carboxylic acids, phenols, proteins and alkaloids can provide electrons to reduce gold into gold nanoparticles. The final configuration depends on the concentration of plant extract, metal salt, pH of the reaction mixture, temperature and incubation time [23]. Usually, the preparation of plant extracts require extra steps. A few examples are presented next (check reference [23,149,150] for a larger

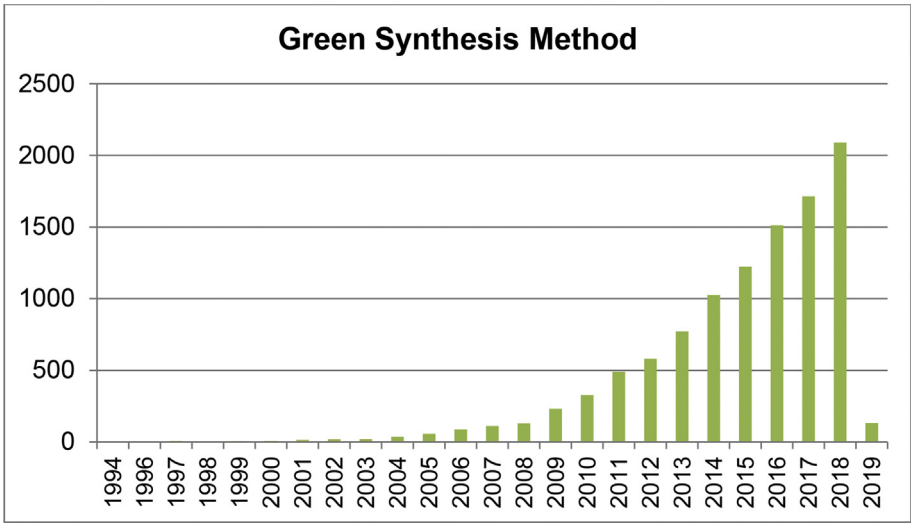

Fig. 12. Number of research articles published using green-synthesis thought the years. (For interpretation of the references to color in this figure legend, the reader is referred to the Web version of this article.)

Table 7
Summary of the papers presented using Ascorbic Acid.

Green Synthesis			
Reference	$HAuCl_4$ (concentration of $HAuCl_4$/volume)	Green product	AuNP size
Jayaseelan [151]	1 mM/60 mL	Abelmoschus esculentus	45–75 nm
Armendariz [152]	errado		
Song [153]	1 mM/190 mL	Magnolia kobus and Diopyros kaki	5–300 nm
Ghosh [154]	0.7 mM	Gnidia glauca flower extract	50–150 nm
Hamelian [155]	1 mM/100 mL	Thyme plant	6–26 nm
Ahmad [156]	12.69 mM/100 mL	Elaeis guineensis (palm oil)	8.22 nm
Nazirov [157]	0.01 M	imidazole derivative of chitosan	2.3 nm
Taib [158]	5 mM/5 mL	Hibiscus sabdariffa	of 9 ± 3
Selvi [159]	1 mM	Gum kondagogu obtained from Cochlospermum gossypium	4.08–12.73 nm
Nagalingam [160]	1 mM/20 mL	A. bettzickiana	80–120 nm
Sonia [161]	1 mM/10 mL	chitosan	10–15 nm
Kumar [162]	1mM/90 mL	Croton Caudatus Geisel	10.75 nm
Ponnanikajamideen [163]	1 mM	Chamaecostus cuspidatus	50 nm
Vilmaraj [164]	1 mM/40 mL	M. indica	46.8 nm
Rajan [165]	2.5×10^{-4} M/30 mL	Elettaria cardamomum	15.2 nm
Rajan [166]	2.5×10^{-4} M/30 mL	Areca catechu	22.2 nm – room temperature 18.1 nm - 100 °C
Vilas [167]	2.49×10^{-4} M/40 mL	Coleus aromaticus	28 nm
Vilas [168]	2.5×10^{-4} M/40 mL	Myristica fragrans	29 nm
Aromal [169]	2.5×10^{-4} M/30 mL	Benincasa hispida	10 nm - 30 nm
Aswathy [170]	1.3×10^{-4} M/50 mL	tannic acid	10 nm
Philip [171]	5×10^{-4} M/30 mL	Hibiscus extract	14 nm
Suvith [172]	2×10^{-4} M/10 mL	Guggulutiktham Kashayam	32 nm
Rajan [173]	2.5×10^{-4} M/30 mL	Garcinia Combogia (GC)	12, 16, 21 nm at different volumes of GC
Meena Kumari [174]	2.94×10^{-4} M/30 mL	coconut oil	38–49 nm
Aswathy Aromal [175]	1.3×10^{-4} M/30 mL	Trigonella foenum-graecum	20 nm- without pH 18 nm- pH 7
Sheny [176]	2.5×10^{-4} M/30 mL	Anacardium occidentale (AO)	15 nm and 37 nm at different volumes of AO
Aswathy Aromal [177]	2.5×10^{-4} M/30 mL	dasamoolarishtam, ashokarishtam, Jirakarishtam, and amrutharishtam	15 nm, 17 nm, 23 nm, and 20 nm
Aromal [178]	2.5×10^{-4} M/30 mL	Horse gram	14 nm- room temperature 17 nm - 100 °C
Sheny [179]	2.5×10^{-4}M/30 mL	Anacardium occidentale (AO)	6.5 nm - 17 nm at different volumes of AO
Philip [180]	5×10^{-4} M/40 mL	Mangifera indica	17 nm
Smitha [181]	2×10^{-4} M/30 mL	Cinnamomum zeylanicum	25 nm
Philip [182]	42% (w/v)/30 mL	Natural honey	15 nm
Philip [183]	20.8% (w/w)/30 mL	Volvariella volvacea (VV)	from 20 nm to 150 nm at different volumes of VV
Philip [184]	10^{-4} M/20 mL	Tannic acid	9 nm

compilation). Fig. 12 presents the amount of published papers using green-synthesis. Table 7 presents a summary of the papers presented.

Jayaseelan et al. [151] described the synthesis of gold nanoparticles (AuNPs) using seed aqueous extract of Abelmoschus esculentus. A. esculentus seeds were washed thoroughly in tap water and finally rinsed with distilled water until no foreign material remained. The freshly cleaned seeds were left drying for 15 days at room temperature. The dried seeds were pulverized until a powder texture was achieved. The samples were stored in an air tight container and protected from sunlight for further use. Two grams of finely powdered seed was mixed with 100 mL of deionized water and then the mixture was boiled for 30 min, cooled and filtered. The extract was used fresh within 1 h. Aqueous broth of *A. esculentus* seed (40 mL) was added to 60 mL of 1 mM aqueous $HAuCl_4$ solution and the solution was placed in orbital shaker at room temperature, for reduction of Au^{3+} to Au^0. The bio-reduction of the gold ions in the solution was monitored periodically by measuring the UV–visible spectroscopy of the solutions. The reaction rapidly turned ruby red. The optimum time required for the completion of reaction was 10 min. The AuNPs obtained from the solution were purified by repeated centrifugation at 2000 rpm for 10 min followed by dispersion of the pellet thrice in deionized water to remove the water-soluble biomolecules such as proteins and secondary metabolites. The water suspended NPs were frozen at 30 °C overnight and then kept under vacuum for 24 h. The particle size range was determined to be 45–75 nm.

Armendariz et al. [152] produced AuNP by using Avena sativa biomass. A sample of 0.150 g of oat ground stems were weighed and washed twice with 0.1 M HCl and three times with deionized water (DI). The biomass was resuspended in 30 mL of DI water in order to have a final concentration of 5 mg of biomass per mL of solution. Using diluted concentrations of HCl and NaOH, a portion of the biomass suspension was adjusted to pH 2. Subsequently, aliquots of 2.0 mL each were taken and placed into three test tubes. These test tubes were centrifuged for 5 min at 3000 rpm and the supernatants were discarded. Batch of three test tubes were adjusted to pH 3, 4, 5 and 6 using the same method described above. In a separate beaker, a 0.1 mM Au(III) solution was prepared using $KAuCl_4$. The value of pH was adjusted to 2 and three aliquots of 2 mL each were transferred to the test tubes containing the oat biomass. All the test tubes were then agitated for 1 h, followed by centrifugation. The supernatants were separated from the biomass and used for further gold analysis. The smaller nanoparticles and the higher occurrence

of these were observed at pH values of 3 and 4 (5–20 nm), whereas the larger nanoparticles were observed at pH 2 (25 to approximately 85 nm).

Song et al. [153] used leaf extracts of two plants, Magnolia kobus and Diopyros kaki, obtaining particles from 5 to 300 nm (avg 40 nm). Magnolia kobus and Persimmon (D. kaki) leaves were collected and dried for 2 days at room temperature. The plant leaf broth solution was prepared by taking 5 g of thoroughly washed and finely cut leaves in a 300 mL Erlenmeyer flask along with 100 mL of sterile distilled water and then boiling the mixture for 5 min before finally decanting it. The solutions were stored at 4 °C and used within a week. Typically, 10 mL of leaf broth was added to 190 mL of 1 mM aqueous $HAuCl_4$ solution for the reduction of Au^{3+} ions. The gold nanoparticle solution thus obtained was purified by repeated centrifugation at 15,000 rpm for 20 min followed by redispersion of the pellet in deionized water.

Hamelian et al. [155] produced NPs with Thyme. Thyme plant was washed several times with deionized water and dried at 25 °C in the incubator. Then it was powdered to smallest size by a mortar. The obtained powder (2 g) was boiled in 300 mL water for 30 min until the solution color changed to light yellow. The extract was filtered and maintained at 4 °C for further study. For each synthesis, Thyme extract (10 mL) was added to aqueous solution of (1 mM) $HAuCl_4$ (100 mL) at room temperature and stirred. The color of the solution during 30 min turned to dark red (see Fig. 3) that indicated the formation of gold nanoparticles. The solution stirred for 1 h to complete reduction process, then centrifuged at 12,000 rpm for 15 min and upper phase was removed. Next, obtained AuNPs was washed several times with deionized water to remove all uncoordinated biological materials, and finally, it let dry in an oven at 50 °C. Au nanoparticles had diameters between 6 and 26 nm.

Ahmad et al. [156] used Elaeis guineensis (palm oil) leaves extract. Palm oil leaves (OPL) were cleaned with deionized water to remove contaminations deposited on their surfaces. OPL were then sun dried for one week and washed again with deionized water to remove dirt that could have been placed during the drying process. These OPL were oven dried at 70 °C for 8 h and grinded fine OPL powder. Aqueous OPL extract was prepared by adding 5 g of OPL powder in 100 mL deionized water and heating it at 70 °C, stirred at 500 RPM for 10 min followed by gravity filtration. The filtrate was kept in cold storage at 4 °C for further experimentation. A stock solution of gold chloroauric acid (12.69 mM) was made by dissolving 500 mg of gold precursor in 100 mL of deionized water. Stock solution was further diluted with deionized water to prepare 1.53 mM concentration of gold chloroauric acid. AuNPs were biosynthesized at room temperature by mixing 10 mL of aqueous gold chloroauric acid (1.53 mM) and 10 mL of aqueous OPL extract with an addition of 50 mL of deionized water. Average size was 8.22 nm.

Nazirov et al. [157] proposed a one-pot green synthesis using imidazole derivative of chitosan. IMC (N-(4-imidazolyl)methyl-chitosan) stock solutions of a concentration of 0.1% were prepared by dissolution of the required amount of polymer in 0.1% acetic acid solution. $HAuCl_4$ solution of a concentration of 0.01 M was prepared by dissolution of an appropriate amount of gold foil in aqua regia followed by three cycles of evaporation/addition of concentrated HCl. Stock solution of $HAuCl_4$ was added into freshly prepared IMC solutions to obtain Au(III)/IMC(monomer). The mixtures were permanently stirred and kept at 25 °C for at least 7 days. Ultra-small gold nanoparticles of an average diameter of 2.3 nm were observed.

Taib used Hibiscus sabdariffa L. extract as a reduction agent for nanoparticle synthesis. The fresh H. sabdariffa L. were cleaned with distilled water to remove impurities and dried for 2 days at 65 °C. Then, the dried H. sabdariffa L. were grinded into fine powder. Around 1.00 g of the powder was immersed into 100 mL of distilled water for 30 min at 60 °C. The solid content was filtered out, leaving a pale orange color residual extract which has a pH of 3.1. This extract was further used in the synthesis of the AuNPs. About 5 mL aqueous solution of $HAuCl_4$ (5 mM) was mixed with the solution containing 10 mL of H. sabdariffa L. aqueous extract and 10 mL of distilled water under constant stirring of 600 rpm at room temperature. The pale orange color solution becomes purple color which indicates the formation of AuNPs in aqueous solution. Analysis show that the synthesized AuNPs have mean diameter and standard deviation of 9 ± 3 [158].

Gold nanoparticles constructs (GK-AuNPs) was prepared using gum kondagogu (Gk) obtained from Cochlospermum gossypium, a natural biopolymer which acts as both stabilizing and reducing agent. GK samples were powdered in a high-speed mechanical blender and were sieved through a test sieve (mesh size − 45 μm). The GK powder (1.0 g) was accurately weighed and dispensed into a clean plastic beaker containing 100 mL of Milli Q water which was subjected to magnetic stirring at room temperature (298 K) and was gently stirred overnight at 2000 rpm. Then the gum solution was centrifuged at 5000 rpm for 10 min at room temperature (298 K). The supernatant containing the soluble gum solution was freeze-dried and stored at room temperature (298 K) until further use. GK-AuNPs were prepared by means of simple reduction of $HAuCl_4$ with GK in an aqueous condition. Soluble GK (1%) stock solution was prepared by dissolving soluble GK (1 g) in Milli Q (100 mL) water followed by vortexing. After complete dissolution, definite volume of 1 mM $HAuCl_4$ solution was added to 0.5% soluble GK. Later the soluble GK containing $HAuCl_4$ was mixed well and subjected to autoclaving at 121 °C and 15 kg/cm^2 pressure. All the reactions were carried out in autoclavable polypropylene plastic containers. Sizes ranged between 4.08 and 11.73 nm [159].

The plant A. bettzickiana, collected during the month of July from Vellore District, Tamil Nadu, India, is used as a reducing agent in the formations of gold nanoparticles with 80–120 nm by Nagalingam et al. Fresh A. bettzickiana leaves were collected and thoroughly washed with running tap water. Then, the leaves were washed with double distilled water and shade dried up to 5 days. Dried leaves were powdered by using mechanical grinder. Ten grams of the fine leaf powder was mixed with 100 mL of double distilled water. The mixture was boiled at 80 °C for 10 min in boiling water bath and filtered using Whatmann no.1 filter paper. The extract was collected and stored in a refrigerator at 4 °C for further studies. In a typical nanoparticle synthesis procedure, gold solution was prepared by mixing 1 mM of gold chloride ($HAuCl_4$) with 20 mL of double distilled water. About 5 mL of leaf extract was added to 20 mL aqueous gold solution which was heated up to 80 °C for 10 min. Resulted mixture became into cherry red in color after heating. This indicated the reduction of gold metallic (Au^+) ions to gold (Au) nanoparticles [160].

CH-AuNPs were synthesized by using biopolymer chitosan for reduction of gold salt. For preparation, 500 μL of a freshly prepared solution of chitosan (8 mg/mL) dissolved in 1% acetic acid solution was added to 10 mL of 1 mM tetrachloroauric acid ($HAuCl_4$) solution and stirred at 70 °C until the color changed from pale yellow to red, which indicates the nanoparticle formation. Gold NPs had a narrow size distribution with an average size of 10–15 nm [161].

Croton Caudatus Geisel leaf extract was used by Kumar et al. The fresh leaves were individually collected and washed thoroughly with cold water and then with distilled water, up to 10 days shade dried and fine powder was prepared by using mechanical grinder. Two grams of the fine powder was mixed with 200 mL deionized water and boiled for 10 min at 50 °C using a water bath. This was filtered with Whatmann filter paper to get clear aqueous extract. This extract was stored in a refrigerator. Then, chroroauric acid ($HAuCl_4$) was prepared at the 10^{-3} M concentration with double distilled water. Ten milliliters of the leaf extract were mixed with

90 mL of 1 mM chloroauric acid for the synthesis of gold nanoparticles. The color of the mixture is pale yellow initially, after sometime, the color of the reaction mixture changed to dark pink yielding particles with 10.75 nm [162].

Chamaecostus cuspidatus leaves were collected from Horticulture department located in Courtallam, Tirunelveli, Tamilnadu, India by Ponnanikajamideen et al. The leaves were sterilized and washed thoroughly by double distilled water for three times. The clean plant leaves were dried for a week. The dried leaves were then grinded into fine powder. One gram of leaves powder was mixed with 100 mL Erlenmeyer flask and boiled at 80 °C for 20 min. The boiled extract was filtered through Whatman No. 1 filter paper. The collected supernatant was stored at 4 °C in the refrigerator. For gold nanoparticles synthesis, 10 mL of plant powder extract was added in 1 mM of chloroauric acid. The mixtures were kept at room temperature on an orbital shaker. The synthesized nanoparticles are collected by centrifugation and were used for characterization. They had spherical shape with 50 nm average [163].

The seeds of M. indica were chosen to synthesize gold nanoparticles due to its cost effectiveness and vast availability. The dried seeds were chopped into small pieces and powdered using a mechanical blender. Ten grams of seed powder were soaked in 100 mL of distilled water for 5 h under constant stirring at room temperature. The solution was then filtered with Whatman filter paper no.1 and filtrate of the aqueous solution was stored at −20 °C until use. Aliquots of extract were filtered using 0.45 μm filter prior to AuNP's synthesis. Sixty nanometers particles were obtained by combining 40 mL (1 mM) $HAuCl_4 \cdot 4H_2O$ with aqueous M. indica seed extracts (60 mL) at a 6:4 ratio [164].

Two grams of cleaned and dried Elettaria cardamomum (EC) seeds were boiled in 100 mL demineralized water for 5 min and then filtered to obtain the extract. One milliliter of EC extract was added to 30 mL of freshly prepared 2.5×10^{-4} M boiling solution of $HAuCl_4$. The reduction took 2 min and reach a violet shade color. The average particle size of obtained by Rajan et al. particles is 15.2 nm [165].

Fifteen milligrams of Areca catechu (AC) nut powder was boiled in 100 mL demineralized water for 5 min and filtered to get the aqueous extract. To 30 mL of 2.5×10^{-4} M chloroauric acid with pH 6 (at room temperature and 100 °C), 10 mL of the aqueous AC extract was added as a reduction agent, with continued stirring for 5 min. The appearance of a stable violet color indicated the formation of AuNPs. TEM images revealed 22.2 nm and 18.1 nm for the colloids obtained by Rajan et al. at room temperature and 100 °C respectively [166].

Twenty-eight microliters of concentrated Coleus aromaticus (CA) essential oil (extracted from fresh leaf using a Clevenger apparatus) was added by Vilas et al. in 70 mL of acetone to obtain a stock solution. Two milliliters of the stock solution were diluted in 23 mL of a 56.5% ethanol-water. The diluted oil was used as the reductant and surfactant for metallic NPs synthesis. To 40 mL of 2.49×10^{-4} M $HAuCl_4$ solution, 11.5 mL, 15 mL, and 20 mL of the diluted CA oil was added slowly with vigorous stirring at 100 °C, and at pH 7. Higher was the quantity of the bioreductant in each reaction, more reddish the colloid solution became. For 15 mL reaction 28 nm particles were obtained [167].

Vilas et al. used Myristica fragrans (MF) essential oil. One percent was extracted from fresh leaf using the Clevenger apparatus. A stock solution of essential oil-acetone 0.1:15 (v/v) was prepared. One milliliter of this stock solution was diluted in 32 mL of DI water. Particles with 29 nm diameter were obtained by slowly mixing 14 mL of diluted MF oil with 40 mL of a boiling 2.5×10^{-4} M auric chloride solution. The dark red color indicated a full gold reduction [168].

Seeds of Benincasa hispida (BF) fruits were separated, washed and sundried by Aromal et al. Then, 5 g of the dried seed was boiled in 100 mL of water and filtered to obtain pure extract. Gold nanoparticles from 10 nm to 30 nm were prepared by adding 7.5 mL–20 mL of BF seed extract to 30 mL solution of chloroauric acid (2.5×10^{-4} M) at room temperature and 100 °C under vigorous stirring for 2 min [169].

Stable gold colloids with 10 nm ± 2 nm particles were obtained by Aswathy et al. by adding up to 10 mL solution of 6×10^{-3} M tannic acid (purchased from Sigma-Aldrich) to 50 mL a boiling solution of $HAuCl_4$ with concentration of 1.3×10^{-4} M [170].

To get Hibiscus extract, Philip washed the leaves with DI water and then cut. Twenty grams was then stirred with 200 mL DI water for 1 min it at room temperature. The filtrate was used as reducing agent: 5 mL was diluted to 30 mL and mixed with 30 mL $HAuCl_4$ (5×10^{-4} M) solution for 1 min. The particles presented ca. 14 nm of diameter [171].

Guggulutiktham Kashayam (GK), an ayurvedic herbal medicine, was used by Suvith et al. as a reduction agent for metallic AuNPs production. Gold colloid was obtained by adding up to 10 mL of GK to 2×10^{-4} M $HAuCl_4$ at room temperature and also 100 °C. For room temperature AuNPs synthesis took about 1 h for complete reduction of the metal ions, while at 100 °C just 1 min was necessary. TEM micrographs revealed that the size was 15 nm–50 nm (32 nm ca.) [172].

Rajan et al. used dried Garcinia Combogia (GC) fruit as a reducing agent. The extract was washed and then dried. One gram of GC was boiled in 100 mL of deionized water for 3 min. The gold colloids where prepared at 100 °C. In 30 mL of a vigorously stirred aqueous solution of Chloroauric acid (2.5×10^{-4} M), 1, 2, and 10 mL of the extract were added, stirring continued 1 min. One milliliter sample had a size of 21 nm, 2 mL presented 16 nm, and 10 mL the average size was 12 nm [173].

Commercial edible coconut oil of high purity was used by Meena Kumari et al. as reducing agent. A solution of coconut oil and acetone (1:1) was previously prepared. Thirty milliliters of $HAuCl_4$ solution (2.94×10^{-4} M) at boiling temperature was mixed with different volumes (10 mL and 20 mL) of the coconut oil and acetone solution. The TEM images revealed that the average size of particles for 10 mL and 20 mL samples was 49 nm and 38 nm, respectively [174].

Seeds of Trigonella foenum-graecum (also known as Fenugreek) were washed and sun-dried by Aswathy Aromal et al. Ten grams of the dried seeds were boiled in 100 mL of water for 5 min, and then filtered to obtain the pure extract. Four synthesis was performed varying the extract volume (0.5 mL, 1 mL, 2 mL, and 3 mL). The extract was added to 30 mL of $HAuCl_4$ boiling solution (1.3×10^{-4} M). The best result obtained was 3 mL volume without pH adjustment and with pH 7–20 nm and 18 nm, respectively [175].

About 360 g of Anacardium occidentale (AO) fresh leaf were hydrodistilled using Clevenger apparatus, obtaining 0.2 g of oil. The oil was dissolved in 2 mL acetone to form the reducer for the synthesis AuNPs. In 30 mL of aqueous 2.5×10^{-4} M $HAuCl_4$ solution at 100 °C with continuous stirring, 8 mL of oil was added and boiled for 1 min. A reaction with 5 mL at room temperature was also ran. TEM images of AuNPs prepared at room temperature revealed that the particles are mono dispersed and most of them have a hexagonal shape, the average length of it is 36 nm. For 8 mL sample a large number of anisotropic particles were observed by Sheny et al., with sizes varying between 15 nm (triangle shape) and 37 nm (for hexagonal shape) [176].

Four different Arishtams (fermented herbal drink) were purchased in a healthcare centre in India: dasamoolarishtam (DA), ashokarishtam (AK), Jirakarishtam (JA) and amrutharishtam (AM) by Aswathy Aromal et al. A 1% stock solution for each Arishtam was

prepared. Five milliliters of the stock solution were added to 30 mL boiling solution of chloroauric acid (2.5×10^{-4} M). DA, AK JA and AM yielded, respectively, 15 nm, 17 nm, 23 nm, and 20 nm particles [177].

Ten grams of Horse gram (washed and dried) was boiled in 100 mL of water and filtered to obtain an extract. In 30 mL of a 2.5×10^{-4} M $HAuCl_4$ solution, 1 mL Horse gram extract was added. The reduction was performed at room temperature and also at 100 °C. For 1 mL reactions, Aromal et al. obtained 14 nm and 17 nm was obtained at room temperature and 100 °C respectively [178].

Ten grams of homogenized Anacardium occidentale (AC) leaf (washed and dried) were stirred with 100 mL of H_2O for 5 min, and then filtered to obtain the extract. The AC extract (1.25, 2.5, 5 and 10 mL) was added to 30 mL of 2.5×10^{-4} M $HAuCl_4$ solution and then stirred for 1 min to get colloids. The average size was 6.5 nm−17 nm, respectively. The morphology of AuNPs obtained by Sheny et al. was almost spherical [179].

Ten grams of Mangifera indica (MI) fresh leaf was stirred with 100 mL of water at room temperature for 1 min and then filtered. To 40 mL of a 5×10^{-4} M $HAuCl_4$, 20 mL of MI extract was added. This same experiment was repeated using the dried leaf instead of the fresh leaf. The colloid obtained by Philip et al. with the fresh leaf extract presented nanoparticles with 20 nm, while the one that used dried leaf extract presented particles with 17 nm [180].

Twenty-five nanometers particles were obtained by Smitha et al. by using Cinnamomum zeylanicum (CZ) leaf broth as reducing agent. Twenty-four grams of CZ leaf broth (washed and cutted) was added to 300 mL of water, then boiled for 5 min. The nanoparticle synthesis was performed by mixing 30 mL of 2×10^{-4} M aqueous $HAuCl_4$ solution to 4 mL of CZ extract [181].

Colloids with spherical nanoparticles of 15 nm were obtained using Natural honey (obtained by Philip et al. at Kerala Agriculture University) as a reducing agent. A 28% (w/w) honey solution, and a 42% (w/v) $HAuCl_4$ in water solution were prepared for this synthesis. Twenty-five milliliters of the honey solution were added to 30 mL of $HAuCl_4$ solution under vigorous stirring [182].

Volvariella volvacea (VV) mushroom (washed and finely cut) was used by Philip et al. as reducing agent to obtain AuNPs. Sixty-eight grams of VV was boiled for 2 min in 300 mL water and then filtered. In 30 mL of 20.8% (w/w) $HAuCl_4$ the mushroom extract was added varying the volume (6, 8, 10, 12, 14, 16, 18, and 20 mL), at 40 °C and 80 °C. AuNPS from 20 nm to 150 nm were obtained [183].

Philip et al. presented a Tannic acid/citrate reduction. Particles with 9 nm were obtained. The gold solution was a 10^{-4} M $HAuCl_4$ aqueous solution prepared at 60 °C with constant stirring. In 20 mL of water at 60 °C with constant stirring, 0.049 g trisodium citrate, 0.05 g tannic acid and 0.018 g potassium carbonate were added. Both solutions were mixed. After 2 min of boiling a red colloid was observed indicating full gold reduction [184].

4.7. Synthesis by other reducing agents and by other precursors: a few examples

Horisberger used a 1% solution of $HAuCl_4$ (3 mL) then added to distilled water (240 mL) in a clean flask. The solution was neutralized with 0.2 N K_2CO_3 (5.4 mL). An ether solution of white phosphorus (2 mL) was added. The ether solution consisted of 4 parts diethyl ether and 1 part of phosphorus saturated ether. The mixture was shaken and allowed to stand for 15 min at 25 °C. The solution was then heated under reflux for 5 mim and cooled. Particle size was 5.2 nm [185].

Preparation of AuNPs by Ma et al.: 3 mL 0.5 mM cysteine, 2 mL 0.5 mM $HAuCl_4$ was added into a conical flask. After thoroughly mixed for 2 min, the mixed solution was left undisturbed at room temperature (20 °C) for 6 h until the color of the solution changed red and no further color change occurred. The as-prepared sample was first centrifuged twice at 5000 rpm for 8 min, followed by re-dispersion in pure water. At pH 10 particle size was 55 nm [186].

In a typical synthesis, 100 mg of $AuPPh_3Cl$ was mixed with 400 μL of dodecanethiol in 20 mL of toluene to form a clear solution, to which 84 mg of $NaBH_4$ (96%, Sinopharm) was added in one portion. The mixture was heated with stirring at 55 °C for 7 h before the reaction system was cooled to room temperature. AuNPs with 4.9 nm were precipitated out from the reaction mixture as a black solid powder by addition of 40 mL of ethanol. The precipitate was separated by centrifugation before washing with ethanol and natural drying [187].

Particles with 11 nm were obtained by placing 300 mL of 1.0% $NaAuCl_4 \cdot 2H_2O$ was in an Erlenmeyer flask that contained 30 mL of DI water. The mixture was brought to boiling rapidly while stirring. When the mixture came to a boil, 900 μL 1.0% sodium citrate was added. A series of color change was observed from blue, dark purple to final wine red. Purification was achieved by centrifuging at 12,000 rpm for 20 min in 1.5 mL batches in 1.5 mL Eppendorf tubes. The supernatant was discarded, and the sample was redispersed in 1.5 mL pure DI water. The centrifugation as above was repeated twice, and the nanoparticles were stored for further application [188].

Dodecanethiol gold nanoparticles were synthesized by O'Mahony et al. according to the following procedure: $AuCl_3$ (0.1212 g) was dissolved in 13 mL of distilled water. A phase transfer catalyst tetraoctylammonium bromide (TOAB) (0.9645 g) was dissolved in 8.8 mL of $CHCl_3$. The resulting $AuCl_3$ and TOAB solutions were added together and stirred for 1 h at room temperature. This mixture was placed in a 25 mL separating funnel and the $CHCl_3$ layer collected. Dodecanethiol (86 mL) was then added to the stirring $CHCl_3$ solution and stirred further for 5 min $NaBH_4$ (0.1786 g) was then dissolved in 11 mL of distilled water. This aqueous solution was added to the organic solution and the mixture overnight in a 25 mL separating funnel. The resulting $CHCl_3$ phase was then collected and a polar solvent (ethanol) added. The solution was centrifuged at 4500 rpm for 30 min. Centrifuging the $CHCl_3$ phase in the presence of a polar solvent resulted in the precipitation of the dodecanethiol gold nanoparticles from the liquid phase. The nanoparticles with 1−2 nm were reconstituted in hexane, toluene or $CHCl_3$ [189].

Tyagi et al. prepared a reaction mixture by adding $AuCl_3$ (1 mM) to ascorbic acid (10 mM) such that ascorbate to $AuCl_3$ ratio was 7:1. The initial pH of this solution was adjusted to different values of pH values (6, 8 and 10) by adding dilute NaOH or HCl and stirring was done for 2 h at room temperature. Particles presented 36, 31, and 40 nm, respectively [190].

Sadeghi et al. [191] used Stevia rebaudiana leaves extract to produce NPs ranging from 5 to 20 nm. 0.1 g of dried extract of stevia leaf is added into 50 mL deionized water and then stirred for 1 h in a magnetic stirrer at room temperature. Coarse filtering is employed prior to centrifuging the extract at 4000 rpm for 30 min to remove the heavy biomaterials in it. Clear stevia leaf extract is mixed immediately into a 0.1 mM $AuCl_4$ solution of equal volume. Nanoparticles were synthesized ranging between 5 and 20 nm.

4.8. A plus: dendrimers stabilized nanoparticles

Dendrimers are three-dimensional, highly-branched and monodispersed polymeric nanostructures have been used in drug delivery systems [192,193]. They are synthesized via an iterative sequence of reactions such as Michael addition, alkylation and reduction [194,195]. Their shape and macromolecular characteristics allow ideal drug delivery by encapsulating drugs in their interior or covalently conjugating drugs on their surfaces. In

particular, the application of dendrimers as versatile platforms for targeted cancer therapeutics [193].

Golshan et al. [154] synthesized AuNPs by reduction of $HAuCl_4$ in aqueous solution with trisodium citrate and modified with cysteamine to obtain amine-functionalized (Au-NH_2) nanoparticles. Au-NH_2 nanoparticles were used as multifunctional cores and participated in Michael addition of acrylonitrile and reduction process by lithium aluminum hydride (LAH) to synthesize Au-G4A nanoparticles. Also, peripheral primary amine groups of Au-G4A were conjugated with folic acid (FA) (Au-G4F) to study the bioconjugation effect on drug release behavior of nanostructures.

Peters et al. [196] synthesized sulfuric tripodal ligands and tested the reaction stability. In the aqueous phase of a biphasic system, one equivalent of gold salt ($HAuCl_4$) for each sulfur atom in the ligand, dissolved in the organic phase (dichloromethane), was added. This means that 3 equivalents of $HAuCl_4$ were used for the tridentate ligand, 6 equivalents of the gold salt for the hexadentate ligands, and 9 equivalents of gold for the nonadentate. The transfer of the gold salt from the aqueous to the organic phase was achieved by addition of tetra-*n*-octylammonium bromide (TOAB, 2 equivalents with respect to $HAuCl_4$) to the organic phase. Nucleation of the AuNPs was induced via reduction by addition of an aqueous solution of sodium borohydride ($NaBH_4$, 8 equivalents with respect to $HAuCl_4$). Upon addition of the reducing agent, an immediate color change of the organic phase from bright red to opaque dark brown was observed. After rigorous stirring for 15 min, the phases were separated and the particles were precipitated by addition of excess ethanol. Separation of the AuNPs from excess TOAB, $NaBH_4$ and ligand molecules was achieved by centrifugation. A diameter of 1.1 nm was found and further tests showed a single ligand is able to cover and stabilize the entire AuNP.

5. Conclusion

The future for gold nanoparticle is very promising. They can be synthesized by several different routes, with little or no toxicity effects, and unique optical, physicochemical and biological properties. From the data we gathered, a rapid increase in publications is observed. The most used is the Turkevich methodology that yields particles in the 10 nm range.

Given the tremendous potential of colloidal nanogold in current biomedical topics, this review gathered various synthesis methodologies that are being used in reduction of gold ions into gold colloids. All synthesis pathways presented in this paper are valid for producing particles. Small sizes (<10 nm) can be achieve with all techniques, either by filtration methods or as a simple synthesis result (especially in seeding-growth method), living large room for functionalization of other substances, such as drugs or stabilizing agents. The most important factor is that the end result has a narrow size distribution. Also, toxicity of the reagents used in the synthesis must be considered/tested. For example, toluene is toxic, but should the amount used in the Brust-Schiffrin be harmful (probably not)? All new colloids also require further stabilization tests in biological fluids, *in-vitro* and *in-vivo* testing.

The applications of functionalized gold nanoparticles in biotechnology has grown immensely in the last decade raising major concerns about their physiological effects and possible toxicity. The studies published in past few years used a variety of experimental conditions and different protocols producing conflicting results. We are very far from indisputably understanding the nanoparticles toxicological behavior. Correct therapeutic doses, delivery issues (hinder by the protein corona formation) and the inexistence of a toxicity database must be addressed before the technique is largely used. Although they are not toxic, effects like formation of actin filaments, resulting in a decrease in cell proliferation, adhesion, and motility were found in recent studies [197].

Now, optimization and usage-based synthesis is the next step. Among the many challenges being investigated, anti-tumor targeted drug delivery systems and adjuvant treatments are among the most important. Metallic nanosystems in particular have gained vast consideration especially because their size-dependent properties and behavior, enhanced biocompatibility, stability, and oxidation resistance. Because of that fact, they are suitable tools for targeted, controlled and sustained drug release or even to increase external treatment potentials, as they do in radiation therapy. For example, our group in Brazil uses the nuclear radiation as a forming and activation agent for Au^{198}Nps synthesis. Undoubtedly, nanotechnology is/will revolutionize science and gold nanoparticles will occupy a major role in the development of this new field.

Acknowledgement

CDS wish to thank FAPESP-*Fundação de Amparo à Pesquisa do Estado de São Paulo*. Process: 2018/18526-2.

Appendix A. Supplementary data

Supplementary data to this article can be found online at https://doi.org/10.1016/j.jallcom.2019.05.153.

References

[1] M. Adams, Nanoparticles Technology Handbook, NY RESEARCH PRESS, New York, 2015.
[2] M.-C. Daniel, D. Astruc, Gold Nanoparticles: assembly, supramolecular chemistry, quantum-size-related properties, and applications toward biology, catalysis, and nanotechnology, Chem. Rev. 104 (2004) 293–346.
[3] The National Programme on Technology Enhanced Learning (NPTEL, R.J.B. Balaguru, B.G. Jeyaprakash, Electrical & Electronics Engineering – Semiconductor Nanodevices: Introduction to Materials and Classification of Low Dimensional Materials, 2019. https://nptel.ac.in/courses/115106076/Module%205/Module%205.pdf.
[4] D.R. Baer, M.H. Engelhard, G.E. Johnson, J. Laskin, J. Lai, K. Mueller, P. Munusamy, S. Thevuthasan, H. Wang, N. Washton, A. Elder, B.L. Baisch, A. Karakoti, S.V.N.T. Kuchibhatla, D. Moon, Surface characterization of nanomaterials and nanoparticles: important needs and challenging opportunities, J. Vac. Sci. Technol. A Vac. Surf. Films Offic. J. Am. Vac. Soc. 31 (2013), 50820-50820.
[5] J. Zhao, M.H. Stenzel, Entry of nanoparticles into cells: the importance of nanoparticle properties, Polym. Chem. 9 (2018) 259–272.
[6] M. Faraday, The bakerian lecture: experimental relations of gold (and other metals) to light, Phil. Trans. Roy. Soc. Lond. 147 (1857) 145–181.
[7] J. Conde, G. Doria, P. Baptista, Noble metal nanoparticles applications in cancer, J. Drug Deliv. 2012 (2012) 751075.
[8] S. Huang, R. Li, Y. Qu, J. Shen, J. Liu, Fluorescent biological label for recognizing human ovarian tumor cells based on fluorescent nanoparticles, J. Fluoresc. 19 (2009) 1095.
[9] A.Z. Wilczewska, K. Niemirowicz, K.H. Markiewicz, H. Car, Nanoparticles as drug delivery systems, Pharmacol. Rep. 64 (2012) 1020–1037.
[10] M.K. Riley, W. Vermerris, Recent advances in nanomaterials for gene delivery-A review, Nanomaterials (Basel, Switzerland) 7 (2017) 94.
[11] C. Daruich de Souza, E.C.M. Rostelato, A.D.C.C. Gonzalez, B.R. Nogueira, M.A. Fortin, P. Chevallier, New gold nanoparticle synthesis, in: Pannnano- 1st Pan American Congress of Nanotechnology, Guarujá- Brasil, 2017.
[12] P. Chandra, J. Singh, A. Singh, A. Srivastava, R.N. Goyal, Y.B. Shim, Gold nanoparticles and nanocomposites in clinical diagnostics using electrochemical methods, J. Nanoparticles (2013) 12 (2013).
[13] P. Kumar, G. Sharma, V. Gupta, R. Kaur, K. Thakur, R. Malik, A. Kumar, N. Kaushal, O.P. Katare, K. Raza, Oral delivery of methylthioadenosine to the brain employing solid lipid nanoparticles: pharmacokinetic, behavioral, and histopathological evidences, AAPS PharmSciTech 20 (2019) 74.
[14] C.e. Zou, B. Yang, D. Bin, J. Wang, S. Li, P. Yang, C. Wang, Y. Shiraishi, Y. Du, Electrochemical synthesis of gold nanoparticles decorated flower-like graphene for high sensitivity detection of nitrite, J. Colloid Interface Sci. 488 (2017) 135–141.
[15] K. Okitsu, M. Ashokkumar, F. Grieser, Sonochemical synthesis of gold Nanoparticles: effects of ultrasound frequency, J. Phys. Chem. B 109 (2005) 20673–20675.
[16] D. Wostek-Wojciechowska, J. Jeszka, P. Uznanski, C. Amiens, B. Chaudret, P. Lecante, Synthesis of Gold Nanoparticles in Solid State by Thermal

Decomposition of an Organometallic Precursor, 2004.
[17] S.-A. Dong, S.-P. Zhou, Photochemical synthesis of colloidal gold nanoparticles, Mater. Sci. Eng., B 140 (2007) 153–159.
[18] X. Zhang, Z. Sun, Z. Cui, H. Li, Ionic liquid functionalized gold nanoparticles: synthesis, rapid colorimetric detection of imidacloprid, Sens. Actuators B Chem. 191 (2014) 313–319.
[19] X. Huang, I.H. El-Sayed, W. Qian, M.A. El-Sayed, Cancer cell imaging and photothermal therapy in the near-infrared region by using gold nanorods, J. Am. Chem. Soc. 128 (2006) 2115–2120.
[20] T.B. Huff, L. Tong, Y. Zhao, M.N. Hansen, J.-X. Cheng, A. Wei, Hyperthermic effects of gold nanorods on tumor cells, Nanomedicine 2 (2007) 125–132.
[21] P.K. Jain, K.S. Lee, I.H. El-Sayed, M.A. El-Sayed, Calculated absorption and scattering properties of gold nanoparticles of different size, shape, and Composition: applications in biological imaging and biomedicine, J. Phys. Chem. B 110 (2006) 7238–7248.
[22] J.M. Stern, J. Stanfield, Y. Lotan, S. Park, J.-T. Hsieh, J.A. Cadeddu, Efficacy of laser-activated gold nanoshells in ablating prostate cancer cells in vitro, J. Endourol. 21 (2007) 939–943.
[23] K.S. Siddiqi, A. Husen, Recent advances in plant-mediated engineered gold nanoparticles and their application in biological system, J. Trace Elem. Med. Biol. 40 (2017) 10–23.
[24] V. Amendola, R. Pilot, M. Frasconi, O.M. Maragò, M.A. Iatì, Surface plasmon resonance in gold nanoparticles: a review, J. Phys. Condens. Matter 29 (2017) 203002.
[25] K.L. Kelly, E. Coronado, L.L. Zhao, G.C. Schatz, The optical properties of metal Nanoparticles: the influence of size, shape, and dielectric environment, J. Phys. Chem. B 107 (2003) 668–677.
[26] O. Pluchery, H. Remita, D. Schaming, Demonstrative experiments about gold nanoparticles and nanofilms: an introduction to nanoscience, Gold Bull. 46 (2013) 319–327.
[27] S.D. Brown, P. Nativo, J.-A. Smith, D. Stirling, P.R. Edwards, B. Venugopal, D.J. Flint, J.A. Plumb, D. Graham, N.J. Wheate, Gold nanoparticles for the improved anticancer drug delivery of the active component of oxaliplatin, J. Am. Chem. Soc. 132 (2010) 4678–4684.
[28] V.V. Mody, R. Siwale, A. Singh, H.R. Mody, Introduction to metallic nanoparticles, J. Pharm. BioAllied Sci. 2 (2010) 282–289.
[29] R. Raliya, D. Saha, T.S. Chadha, B. Raman, P. Biswas, Non-invasive aerosol delivery and transport of gold nanoparticles to the brain, Sci. Rep. 7 (2017), 44718-44718.
[30] W. Li, X. Zhao, B. Du, X. Li, S. Liu, X.-Y. Yang, H. Ding, W. Yang, F. Pan, X. Wu, L. Qin, Y. Pan, Gold nanoparticle–mediated targeted delivery of recombinant human endostatin normalizes tumour vasculature and improves cancer therapy, Sci. Rep. 6 (2016) 30619.
[31] S.S. Lucky, K.C. Soo, Y. Zhang, Nanoparticles in photodynamic therapy, Chem. Rev. 115 (2015) 1990–2042.
[32] P. Garcia Calavia, G. Bruce, L. Perez-Garcia, D.A. Russell, Photosensitiser-gold nanoparticle conjugates for photodynamic therapy of cancer, Photochemical & photobiological sciences, Offic. J. Eur. Photochem. Assoc. Eur. Soc. Photobiol. 17 (2018) 1534–1552.
[33] Y. Zhang, W. Chu, A.D. Foroushani, H. Wang, D. Li, J. Liu, C.J. Barrow, X. Wang, W. Yang, New gold nanostructures for sensor applications: a review, Materials 7 (2014) 5169–5201.
[34] J. Ma, Y. Liu, P.F. Gao, H.Y. Zou, C.Z. Huang, Precision improvement in dark-field microscopy imaging by using gold nanoparticles as an internal reference: a combined theoretical and experimental study, Nanoscale 8 (2016) 8729–8736.
[35] A.C. Wong, D.W. Wright, J.A. Conrad, Functionalized gold nanoparticles for detection of cancer biomarkers, in: V.R. Preedy, V.B. Patel (Eds.), General Methods in Biomarker Research and their Applications, Springer Netherlands, Dordrecht, 2014, pp. 1–26.
[36] N. Chanda, P. Kan, L.D. Watkinson, R. Shukla, A. Zambre, T.L. Carmack, H. Engelbrecht, J.R. Lever, K. Katti, G.M. Fent, S.W. Casteel, C.J. Smith, W.H. Miller, S. Jurisson, E. Boote, J.D. Robertson, C. Cutler, M. Dobrovolskaia, R. Kannan, K.V. Katti, Radioactive gold nanoparticles in cancer therapy: therapeutic efficacy studies of GA-198AuNP nanoconstruct in prostate tumor–bearing mice, Nanomed. Nanotechnol. Biol. Med. 6 (2010) 201–209.
[37] Nanoprobes, Aurovist^{TM} 15 Nm: Gold Blood Pool X-Ray Contrast Agent, 2019. www.nanoprobes.com/products/AuroVist-Gold-X-Ray-Contrast-Agent.html.
[38] Nanoprobes, in: Ni-NTA-Nanogold, 2019. www.nanoprobes.com/products/Ni-NTA-Nanogold-His-tag-labeling-and-detection.html.
[39] P. Zhao, N. Li, D. Astruc, State of the art in gold nanoparticle synthesis, Coord. Chem. Rev. 257 (2013) 638–665.
[40] J. Kimling, M. Maier, B. Okenve, V. Kotaidis, H. Ballot, A. Plech, Turkevich method for gold nanoparticle synthesis revisited, J. Phys. Chem. B 110 (2006) 15700–15707.
[41] C. Schleh, M. Semmler-Behnke, J. Lipka, A. Wenk, S. Hirn, M. Schäffler, G. Schmid, U. Simon, W.G. Kreyling, Size and surface charge of gold nanoparticles determine absorption across intestinal barriers and accumulation in secondary target organs after oral administration, Nanotoxicology 6 (2012) 36–46.
[42] H.E. Toma, V.M. Zamarion, S.H. Toma, K. Araki, The coordination chemistry at gold nanoparticles, J. Braz. Chem. Soc. 21 (2010) 1158–1176.
[43] X. Ji, X. Song, J. Li, Y. Bai, W. Yang, X. Peng, Size control of gold nanocrystals in citrate Reduction: the third role of citrate, J. Am. Chem. Soc. 129 (2007) 13939–13948.
[44] M.S. Bakshi, How surfactants control crystal growth of nanomaterials, Cryst. Growth Des. 16 (2016) 1104–1133.
[45] S. Kumar, Role of Surfactants in Synthesis and Stabilization of Nanoparticles Spectroscopic and Physicochemical Aspects, Panjab University, 2011, p. 218.
[46] M. Brust, M. Walker, D. Bethell, D.J. Schiffrin, R. Whyman, Synthesis of thiol-derivatised gold nanoparticles in a two-phase Liquid-Liquid system, J. Chem. Soc., Chem. Commun. (1994) 801–802.
[47] S. Jain, D.G. Hirst, J.M. O'Sullivan, Gold nanoparticles as novel agents for cancer therapy, Br. J. Radiol. 85 (2012) 101–113.
[48] H. Renner, G. Schlamp, D. Hollmann, H.M. Lüschow, P. Tews, R. Josef, K. Dermann, A. Knödler, Gold, gold alloys, and gold compounds, in: Ullmann's Encyclopedia of Industrial Chemistry, Wiley-VCH, Weinheim, 2005.
[49] U. Schubert, N. Husing, R. Laine, Materials Syntheses: A Practical Guide, Springer, 2008.
[50] T.A. Ali, G.G. Mohamed, E.M.S. Azzam, A.A. Abd-elaal, Thiol surfactant assembled on gold nanoparticles ion exchanger for screen-printed electrode fabrication. Potentiometric determination of Ce(III) in environmental polluted samples, Sens. Actuators B Chem. 191 (2014) 192–203.
[51] R.K. Mohanty, S. Thennarasu, A.B. Mandal, Resveratrol stabilized gold nanoparticles enable surface loading of doxorubicin and anticancer activity, Colloids Surfaces B Biointerfaces 114 (2014) 138–143.
[52] D. Pooja, S. Panyaram, H. Kulhari, S.S. Rachamalla, R. Sistla, Xanthan gum stabilized gold nanoparticles: characterization, biocompatibility, stability and cytotoxicity, Carbohydr. Polym. 110 (2014) 1–9.
[53] P.C. Lee, D. Meisel, Adsorption and surface-enhanced Raman of dyes on silver and gold sols, J. Phys. Chem. 86 (1982) 3391–3395.
[54] A.M. Khalil, V. Georgiadou, M. Guerrouache, S. Mahouche-Chergui, C. Dendrinou-Samara, M.M. Chehimi, B. Carbonnier, Gold-decorated polymeric monoliths: in-situ vs ex-situ immobilization strategies and flow through catalytic applications towards nitrophenols reduction, Polymer 77 (2015) 218–226.
[55] T. Qian, C. Yu, S. Wu, J. Shen, Gold nanoparticles coated polystyrene/reduced graphite oxide microspheres with improved dispersibility and electrical conductivity for dopamine detection, Colloids Surfaces B Biointerfaces 112 (2013) 310–314.
[56] A.C. Jayalekshmi, C.P. Sharma, Gold nanoparticle incorporated polymer/bioactive glass composite for controlled drug delivery application, Colloids Surfaces B Biointerfaces 126 (2015) 280–287.
[57] A. Jebali, F.H.E. Hajjar, S. Hekmatimoghaddam, B. Kazemi, J.M. De La Fuente, M. Rashidi, Triangular gold nanoparticles conjugated with peptide ligands: a new class of inhibitor for Candida albicans secreted aspartyl proteinase, Biochem. Pharmacol. 90 (2014) 349–355.
[58] C.A. Simpson, K.J. Salleng, D.E. Cliffel, D.L. Feldheim, In vivo toxicity, biodistribution, and clearance of glutathione-coated gold nanoparticles, Nanomed. Nanotechnol. Biol. Med. 9 (2013) 257–263.
[59] H. Zhang, L. Ma, P. Li, J. Zheng, A novel electrochemical immunosensor based on nonenzymatic Ag@Au-Fe3O4 nanoelectrocatalyst for protein biomarker detection, Biosens. Bioelectron. 85 (2016) 343–350.
[60] X. Wu, Z. Wei, Q. Liu, T. Pang, G. Wu, Structure and bonding in quaternary AgAuPdPt clusters, J. Alloys Compd. 687 (2016) 115–120.
[61] M.S. Moreno, E. López, M.E. Adrover, N.J. Divins, J. Llorca, CO-PrOx over nano-Au/TiO2: monolithic catalyst performance and empirical kinetic model fitting, Int. J. Hydrogen Energy 41 (47) (2016) 22043–22054.
[62] A.K. Augustine, V.P.N. Nampoori, M. Kailasnath, Rapid synthesize of gold nanoparticles by microwave irradiation method and its application as an optical limiting material, Optik - Int. J. Light Electron Opt. 125 (2014) 6696–6699.
[63] S. Yang, Y. Wang, Q. Wang, R. Zhang, B. Ding, UV irradiation induced formation of Au nanoparticles at room temperature: the case of pH values, Colloids Surf. Physicochem. Eng. Aspects 301 (2007) 174–183.
[64] G.H.C. Varca, S. Kadlubowski, M. Wolszczak, A.B. Lugão, J.M. Rosiak, P. Ulanski, Synthesis of papain nanoparticles by electron beam irradiation – a pathway for controlled enzyme crosslinking, Int. J. Biol. Macromol. 92 (2016) 654–659.
[65] V.V. Malkar, T. Mukherjee, S. Kapoor, Synthesis of silver nanoparticles in aqueous aminopolycarboxylic acid solutions via γ-irradiation and hydrogen reduction, Mater. Sci. Eng. C 44 (2014) 87–91.
[66] M. Murawska, M. Wiatr, P. Nowakowski, K. Szutkowski, A. Skrzypczak, M. Kozak, The structure and morphology of gold nanoparticles produced in cationic gemini surfactant systems, Radiat. Phys. Chem. 93 (2013) 160–167.
[67] S. Jongjinakool, K. Palasak, N. Bousod, S. Teepoo, Gold nanoparticles-based colorimetric sensor for cysteine detection, Energy Procedia 56 (2014) 10–18.
[68] J. Ai, Y. Xu, B. Lou, D. Li, E. Wang, Multifunctional AS1411-functionalized fluorescent gold nanoparticles for targeted cancer cell imaging and efficient photodynamic therapy, Talanta 118 (2014) 54–60.
[69] Y. Zhou, P. Wang, X. Su, H. Zhao, Y. He, Colorimetric detection of ractopamine and salbutamol using gold nanoparticles functionalized with melamine as a probe, Talanta 112 (2013) 20–25.
[70] X. Chen, D. Zhao, Y. An, Y. Zhang, J. Cheng, B. Wang, L. Shi, Formation and catalytic activity of spherical composites with surfaces coated with gold nanoparticles, J. Colloid Interface Sci. 322 (2008) 414–420.
[71] J. Turkevich, P.C. Stevenson, J. Hillier, A study of the nucleation and growth processes in the synthesis of colloidal gold, Discuss. Faraday Soc. 11 (1951) 55–75.

[72] J. Polte, Fundamental growth principles of colloidal metal nanoparticles - a new perspective, CrystEngComm 17 (2015) 6809–6830.
[73] G. Frens, Controlled nucleation for the regulation of the particle size in monodisperse gold suspensions, Nature (1973) 20–22.
[74] T. Yonezawa, T. Kunitake, Practical preparation of anionic mercapto ligand-stabilized gold nanoparticles and their immobilization, Colloids Surf. Physicochem. Eng. Aspects 149 (1999) 193–199.
[75] C.X. Zhang, Y. Zhang, X. Wang, Z.M. Tang, Z.H. Lu, Hyper-Rayleigh scattering of protein-modified gold nanoparticles, Anal. Biochem. 320 (2003) 136–140.
[76] E. Mine, A. Yamada, Y. Kobayashi, M. Konno, L.M. Liz-Marzán, Direct coating of gold nanoparticles with silica by a seeded polymerization technique, J. Colloid Interface Sci. 264 (2003) 385–390.
[77] O. Seitz, M.M. Chehimi, E. Cabet-Deliry, S. Truong, N. Felidj, C. Perruchot, S.J. Greaves, J.F. Watts, Preparation and characterisation of gold nanoparticle assemblies on silanised glass plates, Colloids Surf. Physicochem. Eng. Aspects 218 (2003) 225–239.
[78] Y. Yang, J. Shi, H. Chen, S. Dai, Y. Liu, Enhanced off-resonance optical nonlinearities of Au@CdS core-shell nanoparticles embedded in BaTiO3 thin films, Chem. Phys. Lett. 370 (2003) 1–6.
[79] H. Huang, X. Yang, Chitosan mediated assembly of gold nanoparticles multilayer, Colloids Surf. Physicochem. Eng. Aspects 226 (2003) 77–86.
[80] T. Akiyama, K. Inoue, Y. Kuwahara, N. Terasaki, Y. Niidome, S. Yamada, Particle-size effects on the photocurrent efficiency of nanostructured assemblies consisting of gold nanoparticles and a ruthenium complex–viologen linked thiol, J. Electroanal. Chem. 550–551 (2003) 303–307.
[81] K.C. Grabar, R.G. Freeman, M.B. Hommer, M.J. Natan, Preparation and characterization of Au colloid monolayers, Anal. Chem. 67 (1995) 735–743.
[82] K.S. Mayya, V. Patil, M. Sastry, Lamellar multilayer gold cluster films deposited by the Langmuir–Blodgett technique, Langmuir 13 (1997) 2575–2577.
[83] J.J. Storhoff, R. Elghanian, R.C. Mucic, C.A. Mirkin, R.L. Letsinger, One-pot colorimetric differentiation of polynucleotides with single base imperfections using gold nanoparticle Probes, J. Am. Chem. Soc. 120 (1998) 1959–1964.
[84] I. Ojea-Jiménez, N.G. Bastús, V. Puntes, Influence of the sequence of the reagents addition in the citrate-mediated synthesis of gold nanoparticles, J. Phys. Chem. C 115 (2011) 15752–15757.
[85] N.R. Nirala, P.S. Saxena, A. Srivastava, Colorimetric detection of cholesterol based on enzyme modified gold nanoparticles, Spectrochim. Acta Part A Mol. Biomol. Spectrosc. 190 (2018) 506–512.
[86] K. Mintz, E. Waidely, Y. Zhou, Z. Peng, A.O. Al-Youbi, A.S. Bashammakh, M.S. El-Shahawi, R.M. Leblanc, Carbon dots and gold nanoparticles based immunoassay for detection of alpha-L-fucosidase, Anal. Chim. Acta 1041 (2018) 114–121.
[87] D. Shi, F. Sheng, X. Zhang, G. Wang, Gold nanoparticle aggregation: colorimetric detection of the interactions between avidin and biotin, Talanta 185 (2018) 106–112.
[88] F. Takahashi, N. Yamamoto, M. Todoriki, J. Jin, Sonochemical preparation of gold nanoparticles for sensitive colorimetric determination of nereistoxin insecticides in environmental samples, Talanta 188 (2018) 651–657.
[89] D. Sangamithirai, S. Munusamy, V. Narayanan, A. Stephen, A voltammetric biosensor based on poly(o-methoxyaniline)-gold nanocomposite modified electrode for the simultaneous determination of dopamine and folic acid, Mater. Sci. Eng. C 91 (2018) 512–523.
[90] J. Li, Y. Jiao, Q. Liu, Z. Chen, The aptamer-thrombin-aptamer sandwich complex-bridged gold nanoparticle oligomers for high-precision profiling of thrombin by dark field microscopy, Anal. Chim. Acta 1028 (2018) 66–76.
[91] N. Hanžić, A. Horvat, J. Bibić, K. Unfried, T. Jurkin, G. Dražić, I. Marijanović, N. Slade, M. Gotić, Syntheses of gold nanoparticles and their impact on the cell cycle in breast cancer cells subjected to megavoltage X-ray irradiation, Mater. Sci. Eng. C 91 (2018) 486–495.
[92] L.M. Niu, Y. Liu, K.Q. Lian, L. Ma, W.J. Kang, Characterization of a sensitive biosensor based on an unmodified DNA and gold nanoparticle composite and its application in diquat determination, Arab. J. Chem. 11 (2018) 655–661.
[93] S. Uthaman, H.S. Kim, V. Revuri, J.-J. Min, Y.-k. Lee, K.M. Huh, I.-K. Park, Green synthesis of bioactive polysaccharide-capped gold nanoparticles for lymph node CT imaging, Carbohydr. Polym. 181 (2018) 27–33.
[94] B.B. Karakocak, J. Liang, P. Biswas, N. Ravi, Hyaluronate coating enhances the delivery and biocompatibility of gold nanoparticles, Carbohydr. Polym. 186 (2018) 243–251.
[95] R. Panday, A.J. Poudel, X. Li, M. Adhikari, M.W. Ullah, G. Yang, Amphiphilic core-shell nanoparticles: synthesis, biophysical properties, and applications, Colloids Surfaces B Biointerfaces 172 (2018) 68–81.
[96] P. He, X. Zhu, Phospholipid-assisted synthesis of size-controlled gold nanoparticles, Mater. Res. Bull. 42 (2007) 1310–1315.
[97] L. Hong, M. Lu, M.-P. Dinel, P. Blain, W. Peng, H. Gu, J.-F. Masson, Hybridization conditions of oligonucleotide-capped gold nanoparticles for SPR sensing of microRNA, Biosens. Bioelectron. 109 (2018) 230–236.
[98] R.L. Karpel, M. da Silva Liberato, J.D. Campeiro, L. Bergeon, B. Szychowski, A. Butler, G. Marino, J.F. Cusic, L.C.G. de Oliveira, E.B. Oliveira, M.A. de Farias, R.V. Portugal, W.A. Alves, M.-C. Daniel, M.A.F. Hayashi, Design and characterization of crotamine-functionalized gold nanoparticles, Colloids Surfaces B Biointerfaces 163 (2018) 1–8.
[99] G.S. Perera, S.A. Athukorale, F. Perez, C.U. Pittman, D. Zhang, Facile displacement of citrate residues from gold nanoparticle surfaces, J. Colloid Interface Sci. 511 (2018) 335–343.
[100] B. Bartosewicz, K. Bujno, M. Liszewska, B. Budner, P. Bazarnik, T. Płociński, B.J. Jankiewicz, Effect of citrate substitution by various α-hydroxycarboxylate anions on properties of gold nanoparticles synthesized by Turkevich method, Colloids Surf. Physicochem. Eng. Aspects 549 (2018) 25–33.
[101] J. Wang, S. Mao, H.-F. Li, J.-M. Lin, Multi-DNAzymes-functionalized gold nanoparticles for ultrasensitive chemiluminescence detection of thrombin on microchip, Anal. Chim. Acta 1027 (2018) 76–82.
[102] J. Nebu, J.S. Anjali Devi, R.S. Aparna, B. Aswathy, G.M. Lekha, G. Sony, Fluorescence turn-on detection of fenitrothion using gold nanoparticle quenched fluorescein and its separation using superparamagnetic iron oxide nanoparticle, Sens. Actuators B Chem. 277 (2018) 271–280.
[103] S. Thambiraj, S. Hema, D. Ravi Shankaran, Functionalized gold nanoparticles for drug delivery applications, Mater. Today Proc. 5 (2018) 16763–16773.
[104] P. Kalimuthu, S.A. John, Studies on ligand exchange reaction of functionalized mercaptothiadiazole compounds onto citrate capped gold nanoparticles, Mater. Chem. Phys. 122 (2010) 380–385.
[105] L. Zhao, D. Jiang, Y. Cai, X. Ji, R. Xie, W. Yang, Tuning the size of gold nanoparticles in the citrate reduction by chloride ions, Nanoscale 4 (2012) 5071–5076.
[106] M. Wang, C. Sun, L. Wang, X. Ji, Y. Bai, T. Li, J. Li, Electrochemical detection of DNA immobilized on gold colloid particles modified self-assembled monolayer electrode with silver nanoparticle label, J. Pharm. Biomed. Anal. 33 (2003) 1117–1125.
[107] M. Iqbal, G. Usanase, K. Oulmi, F. Aberkane, T. Bendaikha, H. Fessi, N. Zine, G. Agusti, E.-S. Errachid, A. Elaissari, Preparation of gold nanoparticles and determination of their particles size via different methods, Mater. Res. Bull. 79 (2016) 97–104.
[108] M. Kesik, F.E. Kanik, G. Hızalan, D. Kozanoglu, E.N. Esenturk, S. Timur, L. Toppare, A functional immobilization matrix based on a conducting polymer and functionalized gold nanoparticles: synthesis and its application as an amperometric glucose biosensor, Polymer 54 (2013) 4463–4471.
[109] S. Aryal, B.K.C. Remant, N. Dharmaraj, N. Bhattarai, C.H. Kim, H.Y. Kim, Spectroscopic identification of SAu interaction in cysteine capped gold nanoparticles, Spectrochim. Acta Part A Mol. Biomol. Spectrosc. 63 (2006) 160–163.
[110] Y. Wang, M. Wang, L. Han, Y. Zhao, A. Fan, Enhancement effect of p-iodophenol on gold nanoparticle-catalyzed chemiluminescence and its applications in detection of thiols and guanidine, Talanta 182 (2018) 523–528.
[111] A. Shajkumar, B. Nandan, S. Sanwaria, V. Albrecht, M. Libera, M.-H. Lee, G. Auffermann, M. Stamm, A. Horechyy, Silica-supported Au@hollow-SiO2 particles with outstanding catalytic activity prepared via block copolymer template approach, J. Colloid Interface Sci. 491 (2017) 246–254.
[112] A. Chaudhary, S. Garg, siRNA delivery using polyelectrolyte-gold nanoassemblies in neuronal cells for BACE1 gene silencing, Mater. Sci. Eng. C 80 (2017) 18–28.
[113] C.R. Raj, T. Okajima, T. Ohsaka, Gold nanoparticle arrays for the voltammetric sensing of dopamine, J. Electroanal. Chem. 543 (2003) 127–133.
[114] V. Patil, R.B. Malvankar, M. Sastry, Role of particle size in individual and competitive diffusion of carboxylic acid derivatized colloidal gold particles in thermally evaporated fatty amine films, Langmuir 15 (1999) 8197–8206.
[115] Y.-S. Shon, S. Chuc, P. Voundi, Stability of tetraoctylammonium bromide-protected gold nanoparticles: effects of anion treatments, Colloids Surf. Physicochem. Eng. Aspects 352 (2009) 12–17.
[116] S. Praharaj, S. Panigrahi, S. Basu, S. Pande, S. Jana, S.K. Ghosh, T. Pal, Effect of bromide and chloride ions for the dissolution of colloidal gold, J. Photochem. Photobiol. A Chem. 187 (2007) 196–201.
[117] R.P. Briñas, M. Maetani, J.J. Barchi Jr., A survey of place-exchange reaction for the preparation of water-soluble gold nanoparticles, J. Colloid Interface Sci. 392 (2013) 415–421.
[118] Y. Kuroda, K. Fukumoto, K. Kuroda, Uniform and high dispersion of gold nanoparticles on imogolite nanotubes and assembly into morphologically controlled materials, Appl. Clay Sci. 55 (2012) 10–17.
[119] S.K. Ghosh, Spectroscopic evaluation of 4-(dimethylamino)pyridine versus citrate as stabilizing ligand for gold nanoparticles, Colloids Surf. Physicochem. Eng. Aspects 371 (2010) 98–103.
[120] C. Quintana, P. Atienzar, G. Budroni, L. Mora, L. Hernández, H. García, A. Corma, Development and characterization of fluorine tin oxide electrodes modified with high area porous thin films containing gold nanoparticles, Thin Solid Films 519 (2010) 487–493.
[121] N.M. Vörös, R. Patakfalvi, I. Dékány, Alkylthiol-functionalized gold nanoparticles for sensing organic vapours: the connection between the adsorption isotherm and the sensor resistance, Colloids Surf. Physicochem. Eng. Aspects 329 (2008) 205–210.
[122] L. Zhang, R. Yuan, Y. Chai, X. Li, Investigation of the electrochemical and electrocatalytic behavior of positively charged gold nanoparticle and l-cysteine film on an Au electrode, Anal. Chim. Acta 596 (2007) 99–105.
[123] X. Liu, M. Atwater, J. Wang, Q. Huo, Extinction coefficient of gold nanoparticles with different sizes and different capping ligands, Colloids Surfaces B Biointerfaces 58 (2007) 3–7.
[124] S.W. Kang, J. Hong, J.H. Park, S.H. Mun, J.H. Kim, J. Cho, K. Char, Y.S. Kang, Nanocomposite membranes containing positively polarized gold nanoparticles for facilitated olefin transport, J. Membr. Sci. 321 (2008) 90–93.
[125] Y.Q. Wang, W.S. Liang, A. Satti, K. Nikitin, Fabrication and microstructure of Cu2O nanocubes, J. Cryst. Growth 312 (2010) 1605–1609.

[126] Y.J. Kim, Y.S. Yang, S.-C. Ha, S.M. Cho, Y.S. Kim, H.Y. Kim, H. Yang, Y.T. Kim, Mixed-ligand nanoparticles of chlorobenzenemethanethiol and n-octanethiol as chemical sensors, Sens. Actuators B Chem. 106 (2005) 189–198.
[127] A. Kyrychenko, G.V. Karpushina, S.I. Bogatyrenko, A.P. Kryshtal, A.O. Doroshenko, Preparation, structure, and a coarse-grained molecular dynamics model for dodecanethiol-stabilized gold nanoparticles, Comput. Theor. Chem. 977 (2011) 34–39.
[128] Y.K. Du, J.Z. Xu, M. Shen, P. Yang, L. Jiang, Alkanethiol-stabilized decahedron of gold nanoparticles, Colloids Surf. Physicochem. Eng. Aspects 257–258 (2005) 535–537.
[129] S. Tianimoghadam, A. Salabat, A microemulsion method for preparation of thiol-functionalized gold nanoparticles, Particuology 37 (2018) 33–36.
[130] J.M. Lee, Y.S. Youn, E.S. Lee, Development of light-driven gas-forming liposomes for efficient tumor treatment, Int. J. Pharm. 525 (2017) 218–225.
[131] G.A. Dichello, T. Fukuda, T. Maekawa, R.L.D. Whitby, S.V. Mikhalovsky, M. Alavijeh, A.S. Pannala, D.K. Sarker, Preparation of liposomes containing small gold nanoparticles using electrostatic interactions, Eur. J. Pharm. Sci. 105 (2017) 55–63.
[132] H. Razzaq, R. Qureshi, L. Cabo-Fernandez, D.J. Schiffrin, Synthesis of Au clusters-redox centre hybrids by diazonium chemistry employing double layer charged gold nanoparticles, J. Electroanal. Chem. 819 (2018) 9–15.
[133] M. Brust, G.J. Gordillo, Electrocatalytic hydrogen redox chemistry on gold nanoparticles, J. Am. Chem. Soc. 134 (2012) 3318–3321.
[134] L. Uson, V. Sebastian, M. Arruebo, J. Santamaria, Continuous microfluidic synthesis and functionalization of gold nanorods, Chem. Eng. J. 285 (2016) 286–292.
[135] N.R. Jana, L. Gearheart, C.J. Murphy, Seeding growth for size control of 5–40 nm diameter gold nanoparticles, Langmuir 17 (2001) 6782–6786.
[136] J. Meng, S. Qin, L. Zhang, L. Yang, Designing of a novel gold nanodumbbells SERS substrate for detection of prohibited colorants in drinks, Appl. Surf. Sci. 366 (2016) 181–186.
[137] G.P. Sahoo, D. Kumar Bhui, D. Das, A. Misra, Synthesis of anisotropic gold nanoparticles and their catalytic activities of breaking azo bond in Sudan-1, J. Mol. Liq. 198 (2014) 215–222.
[138] J. Spadavecchia, S. Casale, S. Boujday, C.-M. Pradier, Bioconjugated gold nanorods to enhance the sensitivity of FT-SPR-based biosensors, Colloids Surfaces B Biointerfaces 100 (2012) 1–8.
[139] A. Pan, M. Zhong, H. Wu, Y. Peng, H. Xia, Q. Tang, Q. Huang, L. Wei, L. Xiao, C. Peng, Topical application of keratinocyte growth factor conjugated gold nanoparticles accelerate wound healing, Nanomed. Nanotechnol. Biol. Med. 14 (2018) 1619–1628.
[140] U.M. Nayef, I.M. Khudhair, Synthesis of gold nanoparticles chemically doped with porous silicon for organic vapor sensor by using photoluminescence, Optik 154 (2018) 398–404.
[141] Z. Guo, Y. Wan, M. Wang, L. Xu, X. Lu, G. Yang, K. Fang, N. Gu, High-purity gold nanobipyramids can be obtained by an electrolyte-assisted and functionalization-free separation route, Colloids Surf. Physicochem. Eng. Aspects 414 (2012) 492–497.
[142] Z. Khan, T. Singh, J.I. Hussain, A.A. Hashmi, Au(III)–CTAB reduction by ascorbic acid: preparation and characterization of gold nanoparticles, Colloids Surfaces B Biointerfaces 104 (2013) 11–17.
[143] M.J. Firdhouse, P. Lalitha, Biosynthesis of cubic gold nanoparticles, Int. J. Sci. Eng. Res. 5 (2014). January-2014 1832.
[144] S.C. Boca, M. Potara, F. Toderas, O. Stephan, P.L. Baldeck, S. Astilean, Uptake and biological effects of chitosan-capped gold nanoparticles on Chinese Hamster Ovary cells, Mater. Sci. Eng. C 31 (2011) 184–189.
[145] J. Biswal, S.P. Ramnani, S. Shirolikar, S. Sabharwal, Synthesis of rectangular plate like gold nanoparticles by in situ generation of seeds by combining both radiation and chemical methods, Radiat. Phys. Chem. 80 (2011) 44–49.
[146] J.-H. Lee, K. Kamada, N. Enomoto, J. Hojo, Morphology-selective synthesis of polyhedral gold nanoparticles: what factors control the size and morphology of gold nanoparticles in a wet-chemical process, J. Colloid Interface Sci. 316 (2007) 887–892.
[147] A.S. Patel, S. Juneja, P.K. Kanaujia, V. Maurya, G.V. Prakash, A. Chakraborti, J. Bhattacharya, Gold nanoflowers as efficient hosts for SERS based sensing and bio-imaging, Nano Struct. Nano Objects 16 (2018) 329–336.
[148] A. Jebali, M.H. Anvari-Tafti, Hybridization of different antisense oligonucleotides on the surface of gold nanoparticles to silence zinc metalloproteinase gene after uptake by Leishmania major, Colloids Surfaces B Biointerfaces 129 (2015) 107–113.
[149] J. Santhoshkumar, S. Rajeshkumar, S. Venkat Kumar, Phyto-assisted synthesis, characterization and applications of gold nanoparticles – a review, Biochem. Biophys. Rep. 11 (2017) 46–57.
[150] S. Ahmed, S. Annu, S. Ikram, S. Yudha, Biosynthesis of gold nanoparticles: a green approach, J. Photochem. Photobiol. B Biol. 161 (2016) 141–153.
[151] C. Jayaseelan, R. Ramkumar, A.A. Rahuman, P. Perumal, Green synthesis of gold nanoparticles using seed aqueous extract of Abelmoschus esculentus and its antifungal activity, Ind. Crops Prod. 45 (2013) 423–429.
[152] V. Armendariz, I. Herrera, J.R. peralta-videa, M. Jose-yacaman, H. Troiani, P. Santiago, J.L. Gardea-Torresdey, Size controlled gold nanoparticle formation by Avena sativa biomass: use of plants in nanobiotechnology, J. Nanoparticle Res. 6 (2004) 377–382.
[153] J.Y. Song, H.-K. Jang, B.S. Kim, Biological synthesis of gold nanoparticles using Magnolia kobus and Diopyros kaki leaf extracts, Process Biochem. 44 (2009) 1133–1138.
[154] S. Ghosh, S. Patil, M. Ahire, R. Kitture, D.D. Gurav, A.M. Jabgunde, S. Kale, K. Pardesi, V. Shinde, J. Bellare, D.D. Dhavale, B.A. Chopade, Gnidia glauca flower extract mediated synthesis of gold nanoparticles and evaluation of its chemocatalytic potential, J. Nanobiotechnol. 10 (2012) 17.
[155] M. Hamelian, K. Varmira, H. Veisi, Green synthesis and characterizations of gold nanoparticles using Thyme and survey cytotoxic effect, antibacterial and antioxidant potential, J. Photochem. Photobiol. B Biol. 184 (2018) 71–79.
[156] T. Ahmad, M.A. Bustam, M. Irfan, M. Moniruzzaman, H.M. Anwaar Asghar, S. Bhattacharjee, Green synthesis of stabilized spherical shaped gold nanoparticles using novel aqueous Elaeis guineensis (oil palm) leaves extract, J. Mol. Struct. 1159 (2018) 167–173.
[157] A. Nazirov, A. Pestov, Y. Privar, A. Ustinov, E. Modin, S. Bratskaya, One-pot green synthesis of luminescent gold nanoparticles using imidazole derivative of chitosan, Carbohydr. Polym. 151 (2016) 649–655.
[158] S.H. Mohd Taib, K. Shameli, P. Moozarm Nia, M. Etesami, M. Miyake, R. Rasit Ali, E. Abouzari-Lotf, Z. Izadiyan, Electrooxidation of nitrite based on green synthesis of gold nanoparticles using Hibiscus sabdariffa leaves, J. Taiwan Inst. Chem. Eng. 95 (2018) 616–626.
[159] S. Kalaignana Selvi, J. Mahesh Kumar, R.B. Sashidhar, Anti-proliferative activity of Gum kondagogu (Cochlospermum gossypium)-gold nanoparticle constructs on B16F10 melanoma cells: an in vitro model, Bioactive Carbohydrates Dietary Fibre 11 (2017) 38–47.
[160] N. M, K. V N, D.R. V, P. A, in: Biosynthesis, Characterization, and Evaluation of Bioactivities of Leaf Extract-Mediated Biocompatible Gold Nanoparticles from Alternanthera Bettzickiana, vol. 19, Biotechnology reports, Amsterdam, Netherlands, 2018 e00268-e00268.
[161] Komal Sonia, S. Kukreti, M. Kaushik, Exploring the DNA damaging potential of chitosan and citrate-reduced gold nanoparticles: physicochemical approach, Int. J. Biol. Macromol. 115 (2018) 801–810.
[162] P. Vijaya Kumar, S. Mary Jelastin Kala, K.S. Prakash, Green synthesis of gold nanoparticles using Croton Caudatus Geisel Leaf extract and their biological studies, Mater. Lett. 236 (2018) 19–22.
[163] M. Ponnanikajamideen, S. Rajeshkumar, M. Vanaja, G. Annadurai, In-vivo anti-diabetic and wound healing effect of antioxidant gold nanoparticles synthesized using insulin plant (chamaecostus cuspidatus), Can. J. Diabetes 43 (2) (2018) 82–89.
[164] S. Vimalraj, T. Ashokkumar, S. Saravanan, Biogenic gold nanoparticles synthesis mediated by Mangifera indica seed aqueous extracts exhibits antibacterial, anticancer and anti-angiogenic properties, Biomed. Pharmacother. 105 (2018) 440–448.
[165] A. Rajan, A.R. Rajan, D. Philip, Elettaria cardamomum seed mediated rapid synthesis of gold nanoparticles and its biological activities, OpenNano 2 (2017) 1–8.
[166] A. Rajan, V. Vilas, D. Philip, Studies on catalytic, antioxidant, antibacterial and anticancer activities of biogenic gold nanoparticles, J. Mol. Liq. 212 (2015) 331–339.
[167] V. Vilas, D. Philip, J. Mathew, Biosynthesis of Au and Au/Ag alloy nanoparticles using Coleus aromaticus essential oil and evaluation of their catalytic, antibacterial and antiradical activities, J. Mol. Liq. 221 (2016) 179–189.
[168] V. Vilas, D. Philip, J. Mathew, Phytochemical-capped biogenic gold nanocrystals with chemocatalytic and radical scavenging potential, J. Mol. Liq. 200 (2014) 390–397.
[169] S.A. Aromal, D. Philip, Benincasa hispida seed mediated green synthesis of gold nanoparticles and its optical nonlinearity, Phys. E Low-dimens. Syst. Nanostruct. 44 (2012) 1329–1334.
[170] S. Aswathy Aromal, D. Philip, Facile one-pot synthesis of gold nanoparticles using tannic acid and its application in catalysis, Phys. E Low-dimens. Syst. Nanostruct. 44 (2012) 1692–1696.
[171] D. Philip, Green synthesis of gold and silver nanoparticles using Hibiscus rosa sinensis, Phys. E Low-dimens. Syst. Nanostruct. 42 (2010) 1417–1424.
[172] V.S. Suvith, D. Philip, Catalytic degradation of methylene blue using biosynthesized gold and silver nanoparticles, Spectrochim. Acta Part A Mol. Biomol. Spectrosc. 118 (2014) 526–532.
[173] A. Rajan, M. MeenaKumari, D. Philip, Shape tailored green synthesis and catalytic properties of gold nanocrystals, Spectrochim. Acta Part A Mol. Biomol. Spectrosc. 118 (2014) 793–799.
[174] M. Meena Kumari, D. Philip, Facile one-pot synthesis of gold and silver nanocatalysts using edible coconut oil, Spectrochim. Acta Part A Mol. Biomol. Spectrosc. 111 (2013) 154–160.
[175] S. Aswathy Aromal, D. Philip, Green synthesis of gold nanoparticles using Trigonella foenum-graecum and its size-dependent catalytic activity, Spectrochim. Acta Part A Mol. Biomol. Spectrosc. 97 (2012) 1–5.
[176] D.S. Sheny, J. Mathew, D. Philip, Synthesis characterization and catalytic action of hexagonal gold nanoparticles using essential oils extracted from Anacardium occidentale, Spectrochim. Acta Part A Mol. Biomol. Spectrosc. 97 (2012) 306–310.
[177] S. Aswathy Aromal, K.V. Dinesh Babu, D. Philip, Characterization and catalytic activity of gold nanoparticles synthesized using ayurvedic arishtams, Spectrochim. Acta Part A Mol. Biomol. Spectrosc. 96 (2012) 1025–1030.
[178] S.A. Aromal, V.K. Vidhu, D. Philip, Green synthesis of well-dispersed gold nanoparticles using Macrotyloma uniflorum, Spectrochim. Acta Part A Mol. Biomol. Spectrosc. 85 (2012) 99–104.
[179] D.S. Sheny, J. Mathew, D. Philip, Phytosynthesis of Au, Ag and Au–Ag bimetallic nanoparticles using aqueous extract and dried leaf of Anacardium occidentale, Spectrochim. Acta Part A Mol. Biomol. Spectrosc. 79 (2011)

254–262.
[180] D. Philip, Rapid green synthesis of spherical gold nanoparticles using Mangifera indica leaf, Spectrochim. Acta Part A Mol. Biomol. Spectrosc. 77 (2010) 807–810.
[181] S.L. Smitha, D. Philip, K.G. Gopchandran, Green synthesis of gold nanoparticles using Cinnamomum zeylanicum leaf broth, Spectrochim. Acta Part A Mol. Biomol. Spectrosc. 74 (2009) 735–739.
[182] D. Philip, Honey mediated green synthesis of gold nanoparticles, Spectrochim. Acta Part A Mol. Biomol. Spectrosc. 73 (2009) 650–653.
[183] D. Philip, Biosynthesis of Au, Ag and Au–Ag nanoparticles using edible mushroom extract, Spectrochim. Acta Part A Mol. Biomol. Spectrosc. 73 (2009) 374–381.
[184] D. Philip, Synthesis and spectroscopic characterization of gold nanoparticles, Spectrochim. Acta Part A Mol. Biomol. Spectrosc. 71 (2008) 80–85.
[185] M. Horisberger, J. Rosset, Colloidal gold, a useful marker for transmission and scanning electron microscopy, J. Histochem. Cytochem. 25 (1977) 295–305.
[186] Z. Ma, H. Han, One-step synthesis of cystine-coated gold nanoparticles in aqueous solution, Colloids Surf. Physicochem. Eng. Aspects 317 (2008) 229–233.
[187] W. Hong, X. Yan, R. Li, J. Fan, Gold nanoparticle stabilization within tailored cubic mesoporous silica: optimizing alcohol oxidation activity, Chin. J. Catal. 38 (2017) 545–553.
[188] B. Baruah, T.-A. Miller, Polyoxovanadate fabricated gold nanoparticles: application in SERS, J. Colloid Interface Sci. 487 (2017) 209–216.
[189] T. O'Mahony, V.P. Owens, J.P. Murrihy, E. Guihen, J.D. Holmes, J.D. Glennon, Alkylthiol gold nanoparticles in open-tubular capillary electrochromatography, J. Chromatogr. A 1004 (2003) 181–193.
[190] H. Tyagi, A. Kushwaha, A. Kumar, M. Aslam, pH-dependent synthesis of stabilized gold nanoparticles using ascorbic acid, Int. J. Nanosci. 10 (2011) 857–860.
[191] B. Sadeghi, M. Mohammadzadeh, B. Babakhani, Green synthesis of gold nanoparticles using Stevia rebaudiana leaf extracts: characterization and their stability, J. Photochem. Photobiol. B Biol. 148 (2015) 101–106.
[192] P. Kesharwani, K. Jain, N.K. Jain, Dendrimer as nanocarrier for drug delivery, Prog. Polym. Sci. 39 (2014) 268–307.
[193] J. Zhu, X. Shi, Dendrimer-based nanodevices for targeted drug delivery applications, J. Mater. Chem. B 1 (2013) 4199–4211.
[194] F. Samadaei, M. Salami-Kalajahi, H. Roghani-Mamaqani, Grafting of poly(-acrylic acid) onto poly(amidoamine)-functionalized graphene oxide via surface-mediated reversible addition-fragmentation chain transfer polymerization, Int. J. Polym. Mater. Polym. Biomater. 65 (2016) 302–309.
[195] G. Marzieh, S.K. Mehdi, R.M. Hossein, M. Maryam, Synthesis of poly(-propylene imine) dendrimers via homogeneous reduction process using lithium aluminium hydride: bioconjugation with folic acid and doxorubicin release kinetics, Appl. Organomet. Chem. 31 (2017), e3789.
[196] P.E. Henrik, L. Mario, M. Marcel, Gold nanoparticles stabilized by single tripodal ligands, Part. Part. Syst. Char. 35 (2018) 1800015.
[197] N. Pernodet, X. Fang, Y. Sun, A. Bakhtina, A. Ramakrishnan, J. Sokolov, A. Ulman, M. Rafailovich, Adverse effects of citrate/gold nanoparticles on human dermal fibroblasts, 2006 Jun, Small 2002 (2006), 2766-2073.